

FRI 22/1975

VERSLAG NR. 22

REPORT NO. 1975

VAN 1975

OF _____



U1/E/2/S

BRANDSTOFNAVORSINGSINSTITUUT VAN SUID-AFRIKA

FUEL RESEARCH INSTITUTE OF SOUTH AFRICA

RECOVERY OF MAGNETITE FROM DILUTE SUSPENSIONS IN

ONDERWERP:
SUBJECT: _____

A PILOT PLANT SEPARATOR; DESCRIPTION OF THE MAGNETIC FIELD

PROGRESS REPORT NO 3

ENGINEERING

AFDELING:
DIVISION: _____

P DU TOIT AND AC BONAPACE

NAAM VAN AMPTENAAR:
NAME OF OFFICER: _____

AUTHOR: A.C. BONAPACE AND P. DU TOIT

LEADER OF PROJECT: A.C. BONAPACE

TITLE: RECOVERY OF MAGNETITE FROM DILUTE SUS=
PENSIONS IN A PILOT PLANT SEPARATOR
DESCRIPTION OF THE MAGNETIC FIELD
PROGRESS REPORT NO 3

DIVISION: ENGINEERING

SECTION: HYDROMECHANICS

ENQUIRIES TO: A.C. BONAPACE

RECOVERY OF MAGNETITE FROM DILUTE SUSPENSIONS IN A PILOT PLANT SEPARATOR

DESCRIPTION OF THE MAGNETIC FIELD

PROGRESS REPORT NO 3

BY P. DU TOIT AND A.C. BONAPACE

SYNDOPSIS

Some physical expressions relating the parameters of the magnetic field have been derived.

A description of the magnetic field was carried out by measuring the magnetic flux intensity at various points along the drum circumference and at various radial distances. At each point two components, perpendicular to each other, were measured.

These diagrams were subsequently integrated (by graphical methods) and the magnetic energy content established for the annular space occupied by the slurry.

1. INTRODUCTION

The study of the magnetic field is of fundamental importance for the operation of the magnetic separator.

In this progress report, physical principles and quantitative measurements relevant to the magnetic field investigated, are discussed and presented for subsequent use, particularly in the interpretation of the experimental results.

The subject is covered under the following headings :

- 2) A description of the magnetic field.
- 3) Geometry of the magnetic field of the separator.
- 4) The mechanical force on a particle expressed as a function of the field parameters.

- 5) Detailed calculations relevant to the magnetic energy stored in the annular space through which the slurry flows when undergoing separation.

Previous F.R.I. progress reports dealing with this subject are :-

- a) Progress Report No 1, titled :

"Report on the recovery of magnetite from dilute suspensions in a pilot plant separator", filed as Technical Memorandum No 50 of 1971 and herein referred to as P.R.1.

- b) Progress Report No 2, titled :

"Recovery of magnetite from dilute suspensions in a pilot plant separator", filed as Technical Memorandum No 51 of 1972, and herein referred to as P.R.2.

2. A DESCRIPTION OF THE MAGNETIC FIELD :

In this section the magnetic field is described, while details of the measuring technique and the geometrical constructions used are discussed in sections 3, 4 and 5.

The separation of the magnetite particles takes place in the annular space contiguous to the POLE PIECES and relative to a slurry of low solid concentration (density relative to water 1,03 to 1,07). This space has magnetic properties which can be considered as being equivalent to those of water, which, for all practical purposes are the same as those of a vacuum.

Because of the low magnetite concentration, the distances between the particles are so great that their magnetic interaction may be assumed to be negligible. Consequently, the physics of the magnetic separation can be investigated by using the laws of magnetism applicable to a vacuum and to an isolated particle, considered as an elementary magnet under the influence of the existing field.

Using this approach, the efficiency of the separation has been studied as a function of the magnetic energy content of the space in which the separation takes place.

The /

The obvious advantages of this method are that the field strength and the flux intensity at the various points of the annular space can be measured directly by means of ordinary instruments, and the corresponding energy functions can be calculated by applying the relevant physical laws.

The physical space is described magnetically by

$$B_o = \mu_o H \quad (1) (*)$$

where

B_o is the flux intensity in the vacuum $\left(\frac{V \times s}{m^2}\right)$

H is the magneto motrix force $\left(\frac{A \times \text{turns}}{m}\right)$

and

$\mu_o = 1.256 \times 10^{-6}$ is the induction constant $\left(\frac{V \times s}{\text{Amp} \times m}\right)$

When dealing with a ferromagnetic material such as magnetite, one must introduce the permeability μ (or its susceptibility $\chi = \mu - 1$) symbolically):

$$B = \mu B_o = \mu \mu_o H$$

It is interesting to compare the value of μ_{mag} for magnetite with that of iron (μ_{iron}), e.g. in conditions of saturation, i.e. for a flux intensity :-

$$B = B_{\text{sat.}}$$

Rewriting it as follows :

$$B_{\text{sat. mag}} = \mu_{\text{magn.}} B_o = \mu_{\text{magn.}} \mu_o H$$

$$B_{\text{sat. iron}} = \mu_{\text{iron}} B_o = \mu_{\text{iron}} \mu_o H$$

This yields the following ratios :

For magnetite

$$\frac{B_{\text{sat. magn}}}{B_o} = 95$$

(*) Equations bear the same numbers as those derived analytically in section 4.

$B_{\text{sat.}}$:

For iron

$$\frac{B_{\text{sat. iron}}}{B_0} = 300.$$

Consequently, magnetite particles are considerably less ferromagnetic than iron particles.

The magnetic energy stored in the elementary magnet of unitary volume ($V = 1$), is:

$$e = \frac{E}{V} = \frac{(\mu - 1)^2 B_0^2}{2\mu_0}$$

Where B_0 is the flux density of the field at the point under consideration, and $\mu - 1 = \chi$ is the susceptibility of the elementary magnet.

If the elementary magnet is moved in the direction \vec{x} , i.e. in the direction along which the flux intensity has a component B_{0x} and e.g. against the forces of the field, the energy required to move it from position x to position x_1 will be

$$w_{x1}^x = (\mu - 1)^2 \{e_x(x) - e_x(x_1)\} \tag{28}$$

where

$$e_x(x) = \frac{B_{0x}^2}{2\mu_0} \tag{25}$$

With regard to the geometry of the field, two directions are of particular importance in our study (cf. figure 1) viz.:

The radial direction \vec{R} and the tangential direction \vec{c} .

The direction \vec{R} corresponds to the migration direction of the particles when separating from the slurry.

The direction \vec{c} corresponds to the tangential conveyance of the particles, i.e. along the circumference in the annular space, to the sludge recovery edge.

With /

With reference to figure 1, the annular space where migration takes place is that space bounded by the inflow edge and overflow port, i.e. the canal occupied by the flowing slurry.

The angular amplitude of the migration section is $\theta = 75^\circ$.

The conveying section is the portion of the annular space between the overflow port and the sludge recovery edge and has an angular amplitude of $\theta = 68^\circ$.

In figure 1, a system of polar co-ordinates has been defined with origin situated at the centre of rotation of the drum. Each point is thus specified by a radius R and an argument θ .

The direction of rotation of the drum had been chosen as positive. The axes of the pole pieces are indicated in the figure in a vertical position, i.e. with an orientation angle $\Omega = 0$.

All the subsequent calculations are referred to a separator 1 meter in width (i.e. in the direction normal to the plane of the figure).

A descriptive representation of the magnetic field and relative magnetic energy is given by means of diagrams but without details of the measuring technique and the geometrical constructions utilized. These are dealt with in sections 3 and 5.

Figure 2 illustrates the flux intensity B_{r1} in the radial direction, plotted as a function of the angle θ and at a constant radial distance $R_1 = 0,31250$ m, corresponding to the drum surface.

Figure 3 illustrates the flux intensity $B_{\theta 1}$ in the tangential direction at the distance $R_1 = 0,3125$ (m), i.e. at the drum surface, as a function of the angle θ .

The diagram was obtained as an extra polation of the diagrams of figures 5 and 7.

In fact, the drum surface was accessible only to the fiat probe of the British Thomson Houston meter and not to the A E G meter (cf. later development), i.e. only radial component measurements were possible at the drum surface.

Figure 4/.....

Figure 4 represents the field intensity B_{oR_2} in the radial direction at a distance $R_2 = 0,3325$ m.

Figure 5 represents the field intensity B_{oc_2} in the tangential direction at the same distance $R_2 = 0,3325$ m.

Figures 6 and 7 represent the field intensity B_{oR_3} and B_{oc_3} in radial and tangential directions respectively, at a distance $R_3 = 0,3425$ m.

It should be noticed that R_3 corresponds to the outer dimension of the annular canal occupied by the slurry.

Figures 8 and 9 represent the field intensities B_{R_4} and B_{c_4} in radial and tangential directions, respectively, at a distance $R_4 = 0,3275$ m, i.e. along a circumference 0,40 mm away from the drum surface.

With the aid of these diagrams one can proceed with the calculation of the specific magnetic energy (J/m^3) and of the specific work (J/m) relative to the annular space occupied by the slurry.

The expressions to be used are eqns. (28) and (25) and refer to a separator 1 meter wide. Thus, according to eqn. (25), the energy relative to elementary magnets of susceptibility $\chi = \mu - 1$, situated within the elementary solid of dimensions :-

$$\Delta c. \Delta R.1$$

is

- a) for the radial component, at a flux intensity having a mean value of B_{oRm} :

$$n(\mu-1)^2 e_{Rm} \Delta c. \Delta R = n (\mu - 1) \frac{B_{oRm}^2}{2\mu_0} \Delta c . \Delta R \frac{(J)}{(m)}$$

- b) for the tangential component of a flux intensity having a mean value B_{ocm}

$$n (\mu - 1)^2 e_{cm} \Delta c . \Delta R = n (\mu - 1)^2 \frac{B_{ocm}^2}{2\mu_0} \Delta c \Delta R \frac{(J)}{(m)}$$

The /

The two expressions can be extended to include all the elementary solids within the annular space by means of a double summation relative to the indices i and j .

The total energy is then given by the two forms :

$$a) \quad w'_R = n (\mu - 1)^2 \sum_i \Delta c_i \sum_j \Delta R_j e_{Rm} \quad \frac{(J)}{(m)} \quad (31a)$$

$$b) \quad w'_C = n (\mu - 1)^2 \sum_i \Delta c_i \sum_j \Delta R_j e_{cm} \quad \frac{(J)}{(m)} \quad (31b)$$

The digrams of Figures 10 and 11 represent w'_R and w'_C for an annular space of width $\Delta R = 0,030$ m. (*)

The interpretation of w'_R and w'_C as a function of the angle θ is as follows :

Given two angular values of the argument θ_1 and θ_2 , the differences

$$a) \quad w'_R (\theta_2) - w'_R (\theta_1)$$

or

$$b) \quad w'_C (\theta_2) - w'_C (\theta_1)$$

represent the work available (as difference of energy levels) between the angular positions θ_2 and θ_1 .

Similar calculations will be used extensively in the correlation of the experimental results.

(*) Complete description of the diagramme of these figures follows in chapter 5.

3. GEOMETRY OF THE MAGNETIC FIELD OF THE SEPARATOR

The preliminary description of the magnetic field in P.R.1 has been supplemented by a more basic representation necessary and sufficient for the correlation of the experimental results, as described below.

A measuring device was developed in order to make accurate determinations of the magnetic field components in different spatial positions.

i) CONSTRUCTION FEATURES OF THE SEPARATOR ELECTRO-MAGNET

A lay-out of the electro-magnet inside the rotating drum is shown in figure 14. It is made of three pole pieces, each consisting of a core, 2, with coils, 3, and mounted on a shaft, 4 which can be turned around its axis. It is therefore possible to swing the assembly to any angle.

Each of the pole pieces is made up of three longitudinal sections, illustrated in figure 14-A. Access to the cooling oil pipes and the electric power cables is via the shaft of the group. The parts are assembled in such a way that the centre line of the magnets is offset 4,8 mm from the centre line of the drum.

(cf. figure 14-B).

ii) INSTRUMENTS

Measurement of the field strength, both at the surface of the drum and in the surrounding space, required the use of two separate instruments, one suitable for surface measurements and the other for space measurements.

The points of measurement were situated on a reference plane P, positioned 170 mm from the side surface of the drum, as shown in figure 14-A. This position was chosen to obtain access for the probes and the measuring instruments.

a) BRITISH /

a) BRITISH THOMSON-HOUSTON MAGNETIC FIELD STRENGTH METER

This instrument operates on the Hall effect principle. The sensing unit consists of a thin flat probe with a Germanium Hall plate at the end.

The probe, and in effect the thin rectangular plate of semiconductor material, is placed in a magnetic field in such a manner that the lines of the force pass through the large faces. A voltage is applied to opposite sides of the plate and a potential difference is generated across the two sides, which is proportional both to the magnetic field strength and to the applied voltage. This instrument was used for measurement of the field at the drum surface.

b) A.E.G. OERSTED METER

The A.E.G. Oersted meter is a more refined and accurate instrument. It operates on the principle of a rotating coil which, when placed in a magnetic field, produces an electromotive force proportional to the local magnetic field strength.

iii) MEASURING RIG

A rig, as schematically shown in figure 15, was constructed as a support for the instruments. The sensing probes of the instruments have to be held firmly in different spatial positions to ensure "constant and reproducible" spatial positions from which measurement of high reproducibility could result.

The rig consists of a clamp unit, 1, which secures the probes of both the instruments. By means of this clamp unit, each probe can be set at various radial distances and then orientated parallel to the drum surface. The clamp unit is provided with wheels, 2, running on a circular rail, 3. Thus a probe can be set at various circumferential positions by means of a graduated quadrant, 4, centred with the drum. This quadrant was provided with a scale of 1° divisions used to indicate the position of the probe.

iv) CONVENTIONS /

iv) CONVENTIONS

The geometrical dimensions used in the description of the magnetic field are shown in figure 1. Angles are measured from the vertical taken as origin. Angles are positive when measured in the direction of rotation of the drum, and negative in the opposite direction. Distances are measured from the axis of the drum in the radial direction.

The polar expansions can be rotated to any angle Ω in both the positive and the negative directions.

The field strength determination was carried out at various radial distances R and angular positions θ , for points lying in the reference plane P and with $\Omega = 0$.

In order to facilitate measurements, the magnet was turned through 180° , i.e. so that the polar expansions were showing upwards. Measurements were made around the circumference of the drum at points lying on the plane P , already shown in figures 14 and 15. Due to the length of the probe of the AEG Oersted meter, it was not possible to conduct measurements at distances greater than 170 mm from the side (cf. figure 15-A) with the instrument mounted on the rig.

Measurements of the magnetic field on plane P included the following radial distances :

A. AT THE DRUM SURFACE (i.e. $R_1 = 0,3125$ m)

The drum surface was cleaned and the flat probe of the B.T.H. magnetic field strength meter was subsequently applied at various points on the drum surface around the circumference (360°). The magnetising current was set at 35 amperes.

The values originally given in gauss were converted to $\frac{\text{volt} \times \text{second}}{\text{metre}^2}$ by means of the conversion factor $1 \frac{\text{V} \times \text{s}}{\text{m}^2} = 10^4$ gauss.

The /

The magnetic flux intensity is plotted versus the angle θ in figure 2.

Only the normal component of the field could be measured with the B.T.H. probe.

B. AT A DISTANCE 20mm FROM THE DRUM SURFACE (i.e. $R_2 = 0,3325$ m)

The rig was set so that the probe of the AEG Oersted meter could be positioned around the drum with its sensing tip on the plane P and at a radial distance 20 mm from the drum surface ($0,3125 + 0,0200 = 0,3325$ m from the drum centre).

Two field components were measured at this distance, viz.

- i) A radial component obtained by orientating the probe so that only the radial component of the field was measured.
- ii) A tangential component, i.e. the component normal to the radius R, i.e. in a position normal to that described in (i) above.

These were conducted at a radius of $R_2 = 0,3325$ m.

Both components were measured using a magnetising current of 35 amperes, and plotted against the angle θ as shown in figures 4 and 5.

C. AT A DISTANCE OF 30 mm FROM THE DRUM SURFACE (i.e. $R_3 = 0,3425$ m)

The same procedure described in B was followed, except that the rig was set to measure at a radial distance of 30 mm from the drum axis. The radial and tangential components were measured once again using a magnetising current of 35 amperes, the results are given in figures 6 and 7.

D. AT A DISTANCE OF 60 mm FROM THE DRUM SURFACE (i.e. $R_4 = 0,3725$ m)

The same procedure was followed and the rig was set to measure at a distance of 60 mm from the drum surface. The radial and tangential components for a 35 A magnetising current are represented in figures 8 and 9.

When /

When the curves shown in figures 2 to 9 are considered, it can be seen that in general the plus area under the curve is not equal to the negative area. This can be attributed to the three-dimensional character of the field, i.e. to the existence of a third component in the axial direction occurs.

Note that the distance of the measuring plane P from the end surface of the drum was only 170 mm (cf. figure 14-A).

As mentioned, this plane was selected for reasons of accessibility.

However, the error involved because of this is generally smaller than the error made in certain graphical evaluations discussed at a later stage (cf. section 3), and can therefore be regarded to be negligible.

SHAPE OF THE FIELD

A schematical picture of the magnetic field in the radial direction is shown in figure 16.

The regions where the radial field strength is conventionally negative, (i.e. inwards) have been separated from the regions of positive radial field strength by means of the contour loci 1, 2, 3 and 4.

The representation covers the annular zone bounded by the radial distances $R_1 = 0,3125$ m and $R_2 = 0,3725$ m.

Some points of the contour loci are also given in terms of their co-ordinates in Table No 1.

The specific magnetic energy (J/m^3) has been calculated for the annular space at various radial distances in figures 17, 18, 19 respectively.

The pattern of calculation in the case of figure 17 is outlined as follows -

The /

The magnetic flux intensity B_{OR_1} in the radial direction (figure 2) and the magnetic flux intensity in tangential direction B_{OC_1} (figure 3) are the field intensity components at the drum surface.

At a certain point P of this surface, of argument θ , the specific energy becomes (cf. eqn 25)

$$e_1(\theta) = \frac{B_{OR_1}^2 + B_{OC_1}^2}{2\mu_0} = \frac{1}{2\mu_0} B_{O1}^2$$

being

$$\vec{B}_{OR_1} + \vec{B}_{OC_2} = \vec{B}_{O1} \quad (\text{Vectorial})$$

The specific magnetic energy relative to circumference of radius $R_{1m} = 0,3225$ m has been derived from figures 10 and 11 simply by scalar addition of diagrams e_{R1m} and e_{cim} respectively.

This operation produced the diagram of figure 18.

Analogously, the specific magnetic energy for the points of the circumference $R_{2m} = 0,3375$ m has been derived by scalar addition of diagrams e_{R2m} and e_{c2m} of figures 12 and 13 respectively.

The resultant diagram, is shown in figure 19.

Finally, the equipotential lines of the specific magnetic energy function inside the annular space have been plotted in figure 20.

Each line is characterized by a constant value of the specific magnetic energy.

The three distances $R_1 = 0,3125$ m; $R_2 = 0,3225$ m and $R_3 = 0,3375$ m correspond to the sections of the magnetic field represented in figures 17, 18 and 19.

Along /

Along the line $R_1 = 0,3125$ one finds the region covered by the central pole piece, i.e. for $\theta = 0 \pm 10^\circ$, and the regions covered by the side pole pieces, i.e. for $\theta = -30^\circ \pm 10^\circ$ and $\theta = 30^\circ \pm 10^\circ$.

There are two points, P_1 and P_2 , at which the specific energy is zero. From these two points the energy increases up to a maximum, e.g. from point P_1 to S_1 , and then decreases again.

S_1 and S_2 are two middle points of the profile; their position on the diagram is purely indicative.

In figure 16, positive and negative fluxes must be equal in the absence of a third component (shown by arrow, a, in figure 13-A).

This was found to be exactly so along the central line of the poles (cf. figure 14-A) and practically so on the whole length of each pole (400 mm). However, in the interspace (trace Q) a certain decrease in flux intensity was measured.

A maximum decrease of 20% was measured as against the intensity on the corresponding centre line (the probe in this test was kept on the same horizontal line, i.e. moved in the axial direction only).

For all practical purposes this loss does not affect the precision of the experiments, because the slurry-covered section of the separator has dimensions slightly in excess of one polar expansion length.

SATURATION

The magnetisation curve of the magnetic circuit was investigated at two angles, viz. $\theta = 2,5^\circ$ and $\theta = -30^\circ$, i.e. corresponding to the central and side polar expansions respectively. Measurements were performed at the surface of the drum (i.e. $R = 0,3125$ m) using the BTH magnetic field strength meter, and at various magnetising currents.

This /

This was done by initially increasing the current in a stepwise fashion to the maximum value and then decreasing it stepwise back to zero.

Figures 21 and 22 show the resulting curves at angles of $\theta = -2,5^\circ$ and -30° respectively. Both figures show the effect of saturation occurring at magnetising current values in excess of 20 amperes.

The degree of saturation is expressed in calculations as the deviation from the standard reference straight line shown in figure 21.

4. EXPRESSION OF THE MECHANICAL FORCE ON A PARTICLE AS A FUNCTION OF THE FIELD PARAMETERS

Using the S.I. system of units given in the nomenclature (see appendix), the field strength H , and the flux density B , are related in a vacuum, and with good approximation in air, by the following simple relationship :

$$B_0 = \mu_0 H \quad (1)$$

where μ_0 is the so-called "induction constant" of value :

$$\mu_0 = 1,256 \times 10^{-6} \frac{(V \times s)}{(A \times m)}$$

In the presence of a solenoid of constant section and great length (cf. figure 22), the field strength H is expressed by the ampere turns NI of the solenoid, divided by the coil length ℓ , as

$$H = \frac{NI}{\ell} \quad (2)$$

H is obviously the field strength, measured inside the solenoid, where the field is approximately uniform.

Considering the flux density B_0 and the cross section A of the solenoid, one can express the magnetic flux ϕ as follows :

$$\phi = B_0 A \quad (3)$$

Substitution /

Substitution of (1) and (2) into (3) yields

$$\phi = A \mu_o H = \frac{A}{l} \mu_o NI$$

or

$$\phi \frac{l}{A} \frac{1}{\mu} = NI \tag{4}$$

A well-known expression relates the flux ϕ and the magnetomotive force NI in a vacuum, in a form analogous to the Ohm law for electrical conductors, by means of the factor :-

$$\frac{l}{A} \cdot \mu_o$$

sometimes termed the "magnetic reluctance".

Considering a uniform magnetic flux ϕ obtained, e.g. as in figure 23, by means of two polar expansions in line and a rectangular single spiral coil through which a current I flows, the coil undergoes a mechanical moment M proportional to the product of the current I and the flux ϕ , linked with the coil.

In symbols

$$M = \phi I = 2r \ l B_o I \tag{5}$$

where

$$\phi = 2r l B_o \tag{6}$$

$2r l$ is the cross section of the coil.

Let us define as magnetic moment M' the mechanical moment of the coil linked with to flux density of unitary value.

From (5) and (6)

$$M' = \frac{M}{B_o} = 2r l NI \tag{1 turn} \tag{7a}$$

and for a coil with N turns.

$$M' = \frac{M}{B_o} = 2r l NI \tag{N turns} \tag{7b}$$

If /

If p is the number of the turns per unit of length and ℓ the length of the coil

$$N = p\ell \quad (8)$$

So far one has considered magnetic circuits in a vacuum or in a medium similar to air with characteristics very much like those of a vacuum.

If the space supporting the magnetic circuit is made of a ferromagnetic material such as a solenoid with coils wound around a toroidal ring of iron, then for the same magnetomotive force NI a much larger flux intensity ($B \gg B_0$) is present.

Let us define as magnetic polarisation J the excess flux intensity present in the iron, i.e.

$$J = B - B_0 = (\mu - 1) B_0 \quad (9)$$

where

$$\frac{J}{B_0} = \mu - 1 = \chi \quad (10)$$

is the so-called susceptibility and μ the magnetic permeability (χ and μ being dimensionless and where μ may vary for various ferrous alloys from 100 to a few thousand).

Substitution of (8) into (7b) yields :

$$M' = 2\ell^2 r p I \quad (11)$$

and combined with eqn (2)

$$pI = \frac{NI}{\ell} = H$$

and expressing the volume V as

$$2\ell^2 r = V \quad (12)$$

one obtains for the magnetic moment M' of eqn (7a) and (7b) :

$$M' = VH \quad (13)$$

An elementary rod-like magnet, simulating e.g. a small particle made of a material with permeability μ , if placed in a vacuum in the presence of a flux intensity B_0 , polarises an excess flux J , i.e. :

$$J = B - B_0 = (\mu - 1) B_0$$

which according to (1) and (13) corresponds to a field strength

$$H = \frac{\mu - 1}{\mu_0} \quad B_0 = \frac{M'}{V} \quad (14)$$

i.e.
$$M' = V \frac{\mu - 1}{\mu_0} \quad B_0 = \mu H \quad (15a)$$

Eqn (15a) now expresses the magnetic moment pertinent to the elementary magnet of volume V and permeability μ , when placed in a vacuum.

If the elementary magnet is situated in a medium different from a vacuum, e.g. water, as happens in practice in the case of a particle of magnetite carried in a slurry which flows through a channel occupied by the lines of a magnetic field, eqn (15a) has to be modified as follows :

$$M' = V (\mu_w - 1) \frac{B_{ow}}{\mu_{ow}} \quad (15b)$$

where the permeability relative to the water is now μ_w while B_{ow} and μ_{ow} are the flux intensity and the induction constant relative to the water.

For practical purposes, eqns (15a) and (15b) will be considered as coincident, i.e. eqn (15a) will always be used.

Considering the magnetic energy stored in the space of volume V obtained by slowly increasing the magnetic force from zero to the value H , and the flux intensity from zero to the value $B_0 = \mu_0 H$, one obtains the well-known expression :

$$E = \frac{\mu_0}{2} H^2 V = \frac{B_0^2}{2\mu_0} V \quad (16)$$

The excess magnetic energy stored inside the elementary magnet of volume V and permeability μ will consequently be :

$$E = \frac{(\mu - 1) B_o^2}{2\mu_o} V \quad (17)$$

If $J = (\mu - 1)B_o$ is the polarisation and $\frac{\mu - 1}{\mu} B_o$ the corresponding field strength, its product by B_o yields eqn (17).

Let us define the force \vec{F}^x on a body of volume V and relative permeability μ , immersed in a medium of induction constant μ_o , as the gradient of the energy E in the direction x .

In symbols from eqn (17)

$$\vec{F}^x = \frac{\delta}{\delta \vec{x}} \frac{\mu - 1}{\mu_o} B_o V \frac{\delta (\mu - 1) B_o}{\delta \vec{x}} \quad (18)$$

Taking into consideration eqns (14) and (15), one obtains

$$\vec{F}^x = M' \frac{\delta (\mu - 1) B_o}{\delta \vec{x}} \quad (19)$$

Because of (12), this equation is also valid for a parallelepiped of volume $2 r l^2$.

Considering a sphere of diameter d and volume V such that

$$\frac{\pi d^3}{6} = V = 2 r l^2$$

one can introduce, for the sphere, a form factor φ , and compare its magnetic moment with that of a parallelepiped of equal volume, as follows :

$$M'_{\text{sphere}} = \varphi M'_{\text{Parallelepiped}} \quad (20)$$

Then the mechanical force relative to the spherical particle will be :

$$\vec{F}^x_{\text{sphere}} = \varphi M'_{\text{parallelp.}} \frac{\delta (\mu - 1) B_o}{\delta \vec{x}} \quad (21)$$

The /

The force is proportional to the local gradient of the field strength. This case is similar to the situation of a sphere placed on an incline, undergoing a force proportional to the gradient of the gravitational field at that point, i.e. to the slope of the incline.

However, while the gravitational field exerts a force of constant intensity (at any point of the incline), this is not true, generally speaking, of the magnetic field because B_0 , i.e. M' , is a quantity which varies from point to point and so does its gradient.

For this reason, expression (21) is of more theoretical than practical interest because of the difficulty in the evaluation of B_0 and of its gradient at a point. Nevertheless, it provides a clear physical definition of the mechanical force produced on a particle of matter seen as an elementary magnet by the applied magnetic field.

In the calculation of the work done by the forces of the field in separating the particles of magnetite from the liquid, let us consider at first the elementary energy δE available for moving the particle through a distance δx in the direction of the force \vec{F} .

The elementary work, δW , can be expressed by the following scalar product :

$$\delta W = \vec{F} \cdot \delta \vec{x} = \frac{\delta E}{\delta x} \cdot \delta x \quad (J) \quad (22)$$

For a particle of parallelepipedic form, \vec{F} is given by eqn (19).

This equation contains the magnetic moment M' expressed, in turn, by eqn (15a).

For a correct interpretation of eqns (15a) and (19) in a case where the directions of the vector B and H do not coincide, one must consider their scalar product $B.H$. (*)

(*) Note that for a spherical particle the scalar product is simply given by the ordinary product of the moduli $B H$, because for the sphere the orientation of the two vectors B and H always coincides.

Moreover /

Moreover, if the force \vec{F}^x is required in another (particular) direction x , one has to consider the scalar product of their components \vec{B}^x and \vec{H}^x in the direction x (i.e. B_{ox} and $H_x = (\frac{\mu - 1}{\mu_0})B_{ox}$) and compute the gradient along x .

Then one gets :

$$\vec{F}^x = V \frac{\mu - 1}{\mu_0} B_{ox} \frac{\delta((\mu - 1) B_{ox})}{\delta x} \quad (23)$$

Eqn (23) implicitly contains the assumption that the induction constant and permeability for water and a vacuum are practically the same (i.e. $\mu_0 \approx \mu_{ow}$; $\mu \approx \mu_w$).

Because of eqn (1) one can write

$$\vec{f}^x = \frac{\vec{F}^x}{V} = (\mu - 1)^2 \frac{\delta(\frac{1}{2} B_{ox} H_x)}{\delta x} = \frac{(\mu - 1)^2}{\delta x} \delta \left(\frac{B_{ox}^2}{2\mu} \right) \quad (24)$$

where $\mu - 1$ is again the susceptibility of the particle, i.e. of the magnetite, and

$$\vec{f}^x = \frac{\vec{F}^x}{V} \quad \left(\frac{\text{kg}}{\text{S}^2 \text{M}^2} \right)$$

is the specific force acting on the elementary magnet of unitary volume. If $e_x \left(\frac{\text{J}}{\text{m}} \right)^3$ is the specific magnetic energy of the space corresponding to the field flux intensity B_{ox} , one can write on the strength of eqn (16)

$$\frac{E_x}{V} = e_x = \frac{B_{ox}^2}{2\mu_0} \quad \left(\frac{\text{J}}{\text{m}} \right)^3 \quad (25)$$

Then eqn (24) becomes :

$$\vec{f}^x = \frac{\vec{F}^x}{V} = (\mu - 1)^2 \frac{\delta e_x}{\delta x} \quad \left(\frac{\text{J}}{\text{m}^4} \right) \quad (26)$$

Finally, the specific elementary work δw_x (i.e. the work done by the specific force as defined previously) required to move the elementary magnet of unitary volume through a distance δx is

$$\delta w_x / \dots\dots$$

$$\delta w_x = (\mu - 1)^2 \frac{\delta e_x}{\delta x} \delta x = \frac{(\mu - 1)^2}{3} \left[e_x(x) - e_x(x_1) \right] \left(\frac{J}{m} \right) \quad (27)$$

Performing the integration between two points x_1 and x , one gets:

$$w_{x_1}^x = (\mu - 1)^2 \int_{x_1}^x \frac{\delta e_x}{\delta x} dx = (\mu - 1)^2 \left[e_x(x) - e_x(x_1) \right] \left(\frac{J}{m} \right) \quad (28)$$

This work is referred to the elementary magnet of unitary volume with magnetic moment M^e .

3. DETAILED CALCULATIONS RELEVANT TO MAGNETIC ENERGY

The description of the magnetic field in the form presented in chapter 2, i.e. obtained from instrument readings, cannot be used directly for the correlation of the test results.

The obtained diagrams are initially transformed into magnetic energy diagrams relative to the space occupied by the slurry.

Because the particles of magnetite are suspended in water at a low concentration, it was implicitly assumed that the weakening of the originally present field by their own field when acting as elementary magnets, i.e. the effect of demagnetisation, could be neglected.

Consequently, eqn (28) can be used for the calculation of the specific work along two particular directions, viz.:

- a) The radial direction R,
- b) The tangential direction c.
- a) CALCULATION OF THE WORK IN THE RADIAL DIRECTION:

With reference to figure 5,

$$R_1 = 0,3125 \text{ m}$$

is the radius of the rotating drum,

$\Delta R = 0,030 \text{ m}$ is the width of the annular space in which the slurry flows.

$$R_3 = R_1 + \Delta R = 0,3425 \text{ m}$$

is the outside radius of the annular space (inside radius of the carter enclosing the magnetic separator).

The circumferential arc c^* is simply expressed by the value of the angle Θ , measured from the vertical, multiplied by the radius R , i.e.:

$$c = \Theta R$$

Then the work done by the forces of the field along the radial direction, between points R_1 and R , and for an angular position Θ of the radius, is given by eqn (28), and in accordance with the following conventions:

Assume that the local concentration of particles for a separator 1 metre wide is

$$n \left(\frac{\text{particles}}{\text{m}^2} \right)$$

Then, an elementary solid of dimensions $\delta R \cdot \delta c \cdot 1$ (m^3) contains $n \cdot \delta R \cdot \delta c \cdot 1$ particles, each of which, if considered as a particle of unitary volume, undergoes a specific force \vec{f} given by eqn (24).

Summing up these effects relative to the individual particles, the total work done by the field between distances R_1 and R and relative to the particles contained within a small segment δc of the circumference, is given by the following expression analogous to eqn (28):

$$\int_{R_1}^R \delta w = (\mu - 1) 2n \int_{R_1}^R \frac{\delta e_R}{\delta R} d^2R \delta c \quad (29)$$

Then, writing

$$* \quad n \int \frac{\delta e_R}{\delta R} \delta R^2 = n \int w_R \delta R$$

$$\text{one obtains } \delta_{w'} = (\mu - 1) \delta c n \int_{R_1}^R w_R \delta R \quad \left(\frac{\text{J}}{\text{m}} \right)$$

where $\delta_{w'}$ is the specific elementary work referring to a section of the separator 1 metre wide.

Extending / ...

(*) Note in this respect that the actual used section of the separator is only 0,45 m wide.

Extending the work done on the particles to all those existing along the segment of circumference between $c_1 = \theta_1 R$ and $c = \theta R$, i.e. adding up all the elementary contributions $R\delta\theta$, one arrives at the following double intergral:

$$w'_{R_1\theta_1}^{R\theta} = n (\mu - 1)^2 \int_{c_1 = \theta_1 R}^{c = \theta R} \delta c \int_{R_1}^R e_R \delta R \left(\frac{J}{m}\right) \quad (30a)$$

Expression (30a) denotes the work w' , i.e. that referring to a unit section of the separator, which is required to move all the particles contained inside a section of amplitude θ of the annular space from the distance R_1 to $R_1 + \Delta R = R$, against the action of the magnetic field. The work, according to the sign of the equation, is conventionally positive.

The specific energy e_R within the integral must be considered a function of θ and R , i.e. $e_R(\theta, R)$.

Eqn (30a) can be written in an approximate form by replacing the operation of integration, \int , with that of summation, Σ , and the infinite small interval δ with the finite interval Δ , as follows:

$$w'_{R_1\theta_1}^{R\theta} = n (\mu - 1)^2 \Sigma_{i=1}^P \Delta c_i \Sigma_{j=1}^Q e_{Rmj}(R, \theta) \Delta R_j \left(\frac{J}{m}\right) \quad (31a)$$

where $e_{Rmj}(R, \theta)$ is the mean value of the specific energy inside the ΔR_j interval.

The practical determination of the specific energy was carried out by means of experimental measurements, and according to the following method:

The flux intensity B_R in the radial direction R was measured at distances

$$R_1 = 0,3125 \text{ m} \quad (\text{cf. figure 2})$$

$$R_2 = R_1 + \Delta R_1 = 0,3125 + 0,02 = 0,3325 \text{ m} \quad (\text{cf. figure 3})$$

$$R_3 = R_2 + \Delta R_2 = 0,3325 + 0,01 = 0,3425 \text{ m} \quad (\text{cf. figure 5})$$

$$R_4 = R_3 + \Delta R_3 = 0,3425 + 0,03 = 0,3725 \text{ m} \quad (\text{cf. figure 7})$$

The / ...

The specific magnetic energy at the various points was calculated from the values of B_{OR} (given in figures 2, 3, 5) by means of the following relationship:

$$\frac{E(R,\theta)}{V} = e(R,\theta) = \frac{1}{2} \frac{B_o^2(R,\theta)}{\mu_o} \left(\frac{J}{m^3} \right)$$

This was done in agreement with eqn (16) and for a point of co-ordinates R and θ . Then the mean value $e_{Rjm}^{(R,\theta)}$ relative to the interval j , e.g.

$j = 1$ i.e. for $\Delta R_1 = 0,02$ m

$j = 2$ i.e. for $\Delta R_2 = 0,01$ m

was calculated by means of the expressions

$$e_{R1m}(R_1,\theta) = \frac{1}{2} \frac{B_{R1}^2 + B_{R2}^2}{2} \cdot \frac{1}{\mu_o} \quad j = 1$$

$$e_{R2m}(R_2,\theta) = \frac{1}{2} \frac{B_{R2}^2 + B_{R3}^2}{2} \cdot \frac{1}{\mu_o} \quad j = 2$$

where $j = 1$ and $j = 2$ it signifies that only two intervals were considered:

$\Delta R_1 = 0,02$ m, $\Delta R_2 = 0,01$ m, their sum $\Delta R_1 + \Delta R_2 = 0,03$ m = ΔR , being the width of the annular channel of the separator (cf. figure 5).

The radial specific energy e_{R1m} was then plotted as a function of the argument θ , as shown in figure 10.

Note that e_{R1m} is a mean value referring to a point at radial distance $R_{1m} = 0,3125 + \frac{0,02}{2} = 0,3225$ m and argument θ .

The radial mean specific energy for the next interval e_{R2m} was calculated in the same way and is shown in figure 12.

In this figure, e_{R2m} refers to a point at radial distance $R_{2m} = 0,3325 + \frac{0,010}{2} = 0,3375$ (m) and argument θ .

In carrying out the summation in eqn (31a), the indices i and j were inverted, i.e. first the summation with respect to i was carried out (by graphical integration), and then the summation with respect to j (this simply by superimposing the two curves obtained by graphical integration).

Consequently, in figures 10 and 12 the following curves are shown:

In fig. 10:
$$\sum_{i=1}^p e_{R1m}(R, \theta) \Delta c_i = w_{R1}^i \left(\frac{J}{m} \right) \quad (32a)$$

In fig. 12:
$$\sum_{i=1}^p e_{R2m}(R, \theta) \Delta c_i = w_{R2}^i \quad (33a)$$

The curve

$$e_{R1m} \Delta R_1 + e_{R2m} \Delta R_2 = w_{R^i} \left(\frac{J}{m} \right) \quad (34a)$$

Eqn (34a) represents the specific work performed, in a separator 1 metre wide, for the migration in the radial direction and against the forces of the field (this due to the conventionally positive sign given) of particles present in unit concentration ($n = 1 \cdot \frac{\text{particles}}{m}$) and for a particle of material having a unitary susceptibility ($u - 1 = 1$).

All of this is in agreement with eqn (31a).

With reference to the scales used in figures 10 and 12, they can be derived as follows:

In figure 10 the specific energy e_{R1m} was plotted on an ordinate scale equal to

$$1 \text{ Division} = 400 \left(\frac{J}{m} \right)$$

The scale of the abscissae is

$$1 \text{ division} = 10^0$$

or in linear distance, being $R_1 = 0,3225 \text{ m}$:

$$1 \text{ division} = 0,3225 \times \frac{10^0}{57,30} = 0,056 \text{ m.}$$

In / ...

In the graphical integration a base (segment A B) equal to 10 divisions of the abscissae was selected.

The scale of the integral diagram relative to the function w'_{R1} , which is referred to a strip $\Delta R1 = 0,02(m)$, becomes:

1 Division of ordinates =

$$= 400 \left(\frac{J}{m^3} \right) \times 0,056 (m) \times 0,02 (m) \times 10 \text{ (base length)}$$
$$= 4,5 \left(\frac{J}{m} \right)$$

The same derivation applies to the scale of curve w'_{R2} of figure 12, which has to be referred to a strip $\Delta R2 = 0,01m$ wide.

In this figure the specific energy curve e_{R2} is represented in a scale:

$$1 \text{ Division of the ordinates} = 200 \left(\frac{J}{m} \right).$$

Moreover, 1 Division of the abscissa = $10^0 = 0,056 m$. The length of the base is $CD=40$ divisions, the strip width = $0,010 m$.

Consequently, the scale of the curve relative to the specific work w'_{R2} becomes

$$200 \left(\frac{J}{m} \right) \times 0,056(m) \times 0,01 (m) \times 40 \text{ (base)} = 4,5 \left(\frac{J}{m} \right)$$

In the scale determination of w'_{R2} of figure 12, a small error was purposely introduced by taking into account $R_1 = 0,3225 m$ instead of $R_2 = 0,3375 m$ in the determination of the abscissae scale (1 division = $0,056 m$).

The objective was to achieve the same scale in both figures 10 and 12 for the work specific functions w'_{R1} , w'_{R2} and $w'_R = w'_{R1} + w'_{R2}$ the error being well within the precision of the graphical integration.

The curve w'_R can be interpreted in a number of ways:

With the polar expansions of the separator placed at an angle $\Omega = 0$, i.e. with polar expansions placed vertically:

The / ...

The magnetic energy available for this position $\Omega = 0$ can be read directly from curve w'_R as the difference between ordinates at $\theta = 0$ and $\theta = -75^\circ$, this value being $w'_R = w'_{R0} - w'_R(-75) = 11,4 - 0,2 = 11,2$ (divisions)

$$\Delta w'_R = 11,2 \times 4,5 = 50,5 \quad \left(\frac{J}{m}\right)$$

When the polar expansions are rotated e.g. of an angle $\Omega = +30^\circ$ (i.e. towards collection), the separation work can be read from w'_R as follows:

The curve is kept fixed, but the abscissae origin is shifted in the negative direction (3 divisions = 30° to the left).

Then the magnetic energy available for separation work is read from w'_R as the difference between ordinates $\theta = -30^\circ$ and $\theta = -105^\circ$, i.e.

$$\Delta w'_R = w'_R(-30^\circ) - w'_R(-105^\circ) = 2,9 \text{ (divisions)}$$

$$\Delta w'_R = 2,9 \times 9 = 26 \quad \left(\frac{J}{m}\right)$$

b) CALCULATION OF THE WORK ALONG THE CIRCUMFERENCE (cf. figure 1)

Eqn (30a) can be transformed into an expression for the specific work in the tangential direction by substitution of e_R with e_c as follows:

$$w'_c \int_{R_1 \theta_1}^{R \theta} = n (\mu - 1)^2 \int_{c_1}^{c_1 + \Delta c} \frac{dc}{R_1} e_c dR \quad \left(\frac{J}{m}\right) \quad (31b)$$

which expresses the specific work w'_c , i.e. that referring to a separator 1 metre wide, required to move the particles contained in a strip of width

$$\Delta R = (R_1 + \Delta R) - R_1, \text{ from the circumferential position } c_1 \text{ to } (c_1 + \Delta c).$$

This work is assumed to be conventionally positive, if performed against the forces of the magnetic field.

By replacing integration with summation, and infinitesimal interval δ with finite intervals Δ , one obtains

$$w'_c / \dots$$

$$w_c^{R\theta} = n (\mu - 1)^2 \sum_{i=1}^p \Delta c_i \sum_{j=1}^q e_{cm} (R, \theta) \Delta R_j \left(\frac{J}{m}\right) \quad (31b)$$

where $e_{cm} (R, \theta)$ is the mean value of the specific energy inside the ΔR_j interval, i.e. measured in the circumferential direction.

The practical determination of the circumferential specific energy was carried out by means of experimental measurements, collected according to the following method:

The flux intensity B_{oc} in the tangential direction was measured at distances:

$$R_2 = R_1 + \Delta R_1 = 0,3325 \text{ m} \quad (\text{cf. figure 4})$$

$$R_3 = R_2 + \Delta R_2 = 0,3425 \text{ m} \quad (\text{cf. figure 6})$$

$$R_4 = R_3 + \Delta R_3 = 0,3725 \text{ m} \quad (\text{cf. figure 8})$$

The specific magnetic energy at various points was calculated from the values of B_{oc} (given in figures 5 and 7) with the same procedure as followed in a) i.e. that used for the radial direction. Mean values $e_{cjm} (R, \theta)$ relative to the interval j were determined for:

$$j = 1 \text{ i.e. for } \Delta R_1 = 0,02 \text{ m}$$

$$j = 2 \text{ i.e. for } \Delta R_2 = 0,01 \text{ m}$$

by means of expression (31b)

$$\text{At } R_{m1} = 0,3125 + \frac{0,02}{2} = 0,3225 \text{ m}$$

$$e_{c1m} (R, \theta) = \frac{1}{2} \frac{B_{oc1}^2 + B_{oc2}^2}{2} \cdot \frac{1}{\mu_o} \quad j = 1$$

$$\text{At } R_{m2} = 0,3325 + \frac{0,01}{2} = 0,3375 \text{ m}$$

$$e_{c2m} (R, \theta) = \frac{1}{2} \frac{B_{oc2}^2 + B_{oc3}^2}{2} \cdot \frac{1}{\mu_o} \quad j = 2$$

One should note from the above expressions that $B_{oc}^2 = 0$ because at $R = R_1 = 0,3125 \text{ m}$ one is in contact with the surface of the rotating drum and here the flux is practically normal to the surface with no component in the tangential direction.

Again the two intervals considered were the same as in case a), i.e.:

$$\Delta R_1 = 0,02 \text{ m}$$

$$\Delta R_2 = 0,010 \text{ m}$$

with their sum $\Delta R_1 + \Delta R_2 = \Delta R = 0,03$ corresponding to the width of the annular space of the separator occupied by the slurry inflow.

The graphical representation of the circumferential specific energy e_{c1m} and e_{c2m} is shown in figures 11 and 13 respectively.

By reversing in eqn (31b) the summation (as done previously in case a) in respect of indices i and j, and by performing $\sum_1^P \Delta c_i$ by graphical integration, the following curves were produced

In fig. 11:

$$\sum_{i=1}^P e_{c1m}(R, \theta) \Delta c_i = w'_{c1} \left(\frac{J}{m^2} \right) \quad (32b)$$

In fig. 13:

$$\sum_{i=1}^P e_{c2m}(R, \theta) \Delta c_i = w'_{c2} \left(\frac{J}{m^2} \right) \quad (33b)$$

Moreover, in figure 11 the curve

$$e_{c1m} \Delta R_1 + e_{c2m} \Delta R_2 = w'_c \left(\frac{J}{m} \right) \quad (34b)$$

was obtained by geometrical superimposition of the individual curves e_{c1m} and e_{c2m} multiplied by the corresponding intervals ΔR_1 and ΔR_2 .

Eqn (34b) represents the specific work performed in a separator 1 m wide for the migration in the tangential direction and against the forces of the field (work with conventionally positive sign) on particles, present in unitary concentration $\left(n = 1 \frac{\text{particles}}{m} \right)$ and for a particle material having unitary susceptibility ($\mu - 1 = 1$).

All this is according to eqn (31b).

With / ...

With reference to the scales used in figures 11 and 13, one can repeat considerations already made for case a) (figure 10 and 12). The scale selected for the specific energy, e_{cm} , is:

in figure 11 for e_{c1m} :

$$1 \text{ division} = 2,5 \times 10^{-4} \left(\frac{V \times s}{m^2} \right) = 200 \left(\frac{J}{m^3} \right)$$

in figure 13 for e_{c2m} :

$$1 \text{ division} = 5 \times 10^{-4} \frac{V \times s}{m^2} = 250 \left(\frac{J}{m^3} \right)$$

The calculation of the scale applicable to the curves obtained by graphical integration, i.e. for w'_{cm} , is as follows:

In figure 11: w'_{c1}

1 division of the ordinates =

$$200 \left(\frac{J}{m^2} \right) \times 0,056 \text{ (m)} \times 0,02 \text{ (m)} \times 40 \text{ (Base EF)} = 9 \left(\frac{J}{m} \right)$$

In figure 13: w'_{c2}

1 division of the ordinates =

$$400 \left(\frac{J}{m^2} \right) \times 0,056 \text{ (m)} \times 0,01 \text{ (m)} \times 80 \text{ (Base GH)} = 9 \left(\frac{J}{m} \right)$$

The diagram, summation of

$$w'_{c1} + w'_{c2} = w'_c$$

is shown in figure 11.

The diagram w'_c can be interpreted in a number of ways:

With the polar expansions at an angle Ω i.e. polar expansions vertical, the section of diagram between the overflow slit ($\theta = 0$) and the sludge recovery edge ($\theta = + 68^\circ$) represent the useful work available for the circumferential transport of the particles.

The magnetic energy available for this separation work is given by the

difference /...

difference between the two ordinates, i.e. at point $\theta = + 68$ and $\theta = 0^{\circ}$, its value being in this case,

$$\Delta w'_c = w'_c(+68) - w'_c(0) = 5,3 \text{ divisions}$$

$$\Delta w'_c = 5,3 \times 4,5 = 24,0 \quad \left(\frac{\text{J}}{\text{m}}\right)$$

In the magnet assembly is rotated of an angle, e.g. $\Omega = 30^{\circ}$ as shown in the upper detail of figure 11, the work for circumferential transport of the particle is computed as follows:

The curve w'_c is kept fixed, but the origin of the abscissae is shifted 30° in the negative direction (3 divisions to the left).

Then the magnetic energy available for the tangential transport work is measured on w'_c between the points $\theta = + 38^{\circ}$ and $\theta = -30^{\circ}$, its value being in this case:

$$\Delta w'_c = w'_c(+38^{\circ}) - w'_c(-30^{\circ}) = 7,1 \text{ divisions}$$

$$\Delta w'_c = 7,1 \times 4,5 = 32 \quad \left(\frac{\text{J}}{\text{m}}\right)$$

- In the calculation of the specific work in the radial and circumferential directions carried out at points a) and b), one has implicitly assumed the following:
- 1) that the radial energy is relevant to the process of separation of the particles from the liquid, i.e. inside the separation section located between the inflow edge and the overflow slit;
 - 2) that the tangential energy is relevant to the transport of recovery of the separated particles, i.e. in the recovery section located between the overflow slit and the recovery edge.

TABLE 1

COORDINATES OF POINTS DEFINING CONTOUR LOCI 1,2,3 AND 4 OF FIGURE 16

Distance from Drum surface	R_i	Locus 1	Locus 2	Locus 4	Locus 3
0	$R_1 = 0,3125m$	-18°	-79°	$+19^\circ$	$+80,5^\circ$
20 mm	$R_2 = 0,3325m$	-32°	-115°	$+ 2^\circ$	$+39^\circ$
30 mm	$R_3 = 0,3425m$	-33°	-120°	$+ 3^\circ$	$+39^\circ$
40 mm	$R_4 = 0,3725m$	-37°	-130°	$+ 2^\circ$	$+42^\circ$

<u>SYMBOLS (S.I. UNIT)</u>		<u>DIMENSIONS</u>
A	area	(m^2)
$B_1 B_0$	flux intensity	$(\frac{V \times s}{m^2})$
c	arc of circumference	(m)
E	Energy	J
e	specific energy	$(\frac{J}{m^3})$
$\frac{f}{f}$	specific force-	$(\frac{N}{m^3})$
I	electrical current	A
F	Force	(N)
J	magnetic polarisation	$(\frac{V \times s}{m^2})$
H	Magnetomotrix Force	$(\frac{A \times \text{turns}}{m})$
l	length	(m)
M	Mechanical moment	(N x m)
M'	magnetic moment	(A x m ²)
n	number of particles per unit of length	$(\frac{1}{m})$
N	Number of turns	
p	number of turns per unit length	$(\frac{1}{m})$
V	Volume	(m ³)
W	Work	(J)
w	specific work	$(\frac{J}{m^2})$
w'	specific work	$(\frac{J}{m})$
μ	magnetic permeability	0
μ_0	induction constant for the vacuum	$(\frac{V \times s}{A \times m})$

ρ	Form factor for sphere	
ϕ	magnetic flux	$(\frac{V \times s}{m})$
χ	susceptibility	-
Ω	Polar expansions orientation angle	
θ	angle	

Note:

$$\mu_0 = 1,256 \times 10^{-6} \quad (\frac{V \times s}{A \times m})$$

$$1 \quad \frac{A}{m} = 4 \pi \times 10^{-3} \quad \text{oersted}$$

$$1 \quad \frac{V \times s}{m} = 10^4 \quad \text{gauss}$$

A means ampere

J means joule

N means newton

V means volt

P DU TOIT

RESEARCH OFFICER

A C BONAPACE

PRINCIPAL RESEARCH OFFICER

PRETORIA

17th September, 1975

ACB/PDT/AdP/ER

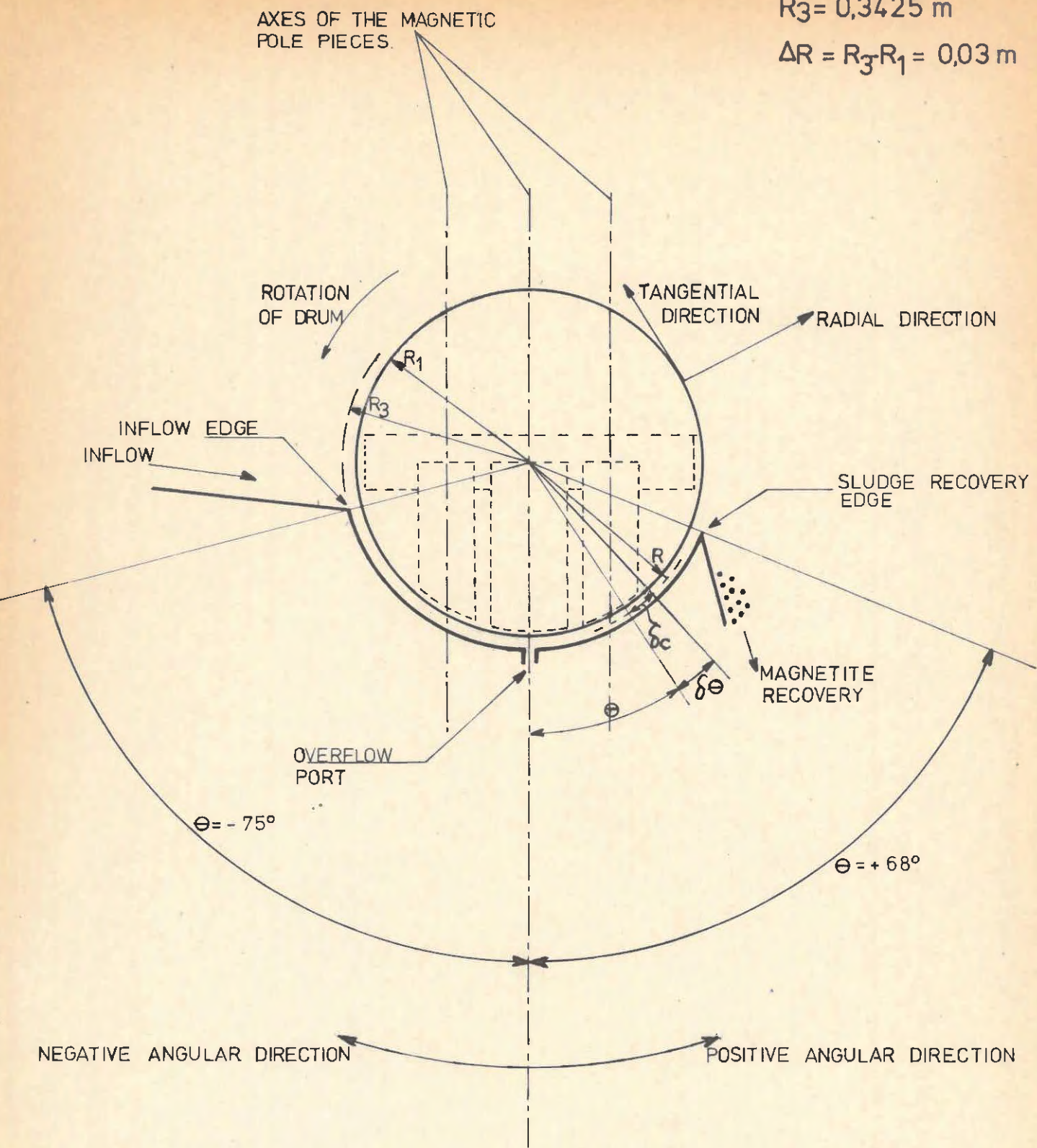
NOTE:

$R_1 = 0,3125 \text{ m}$

$R_3 = 0,3425 \text{ m}$

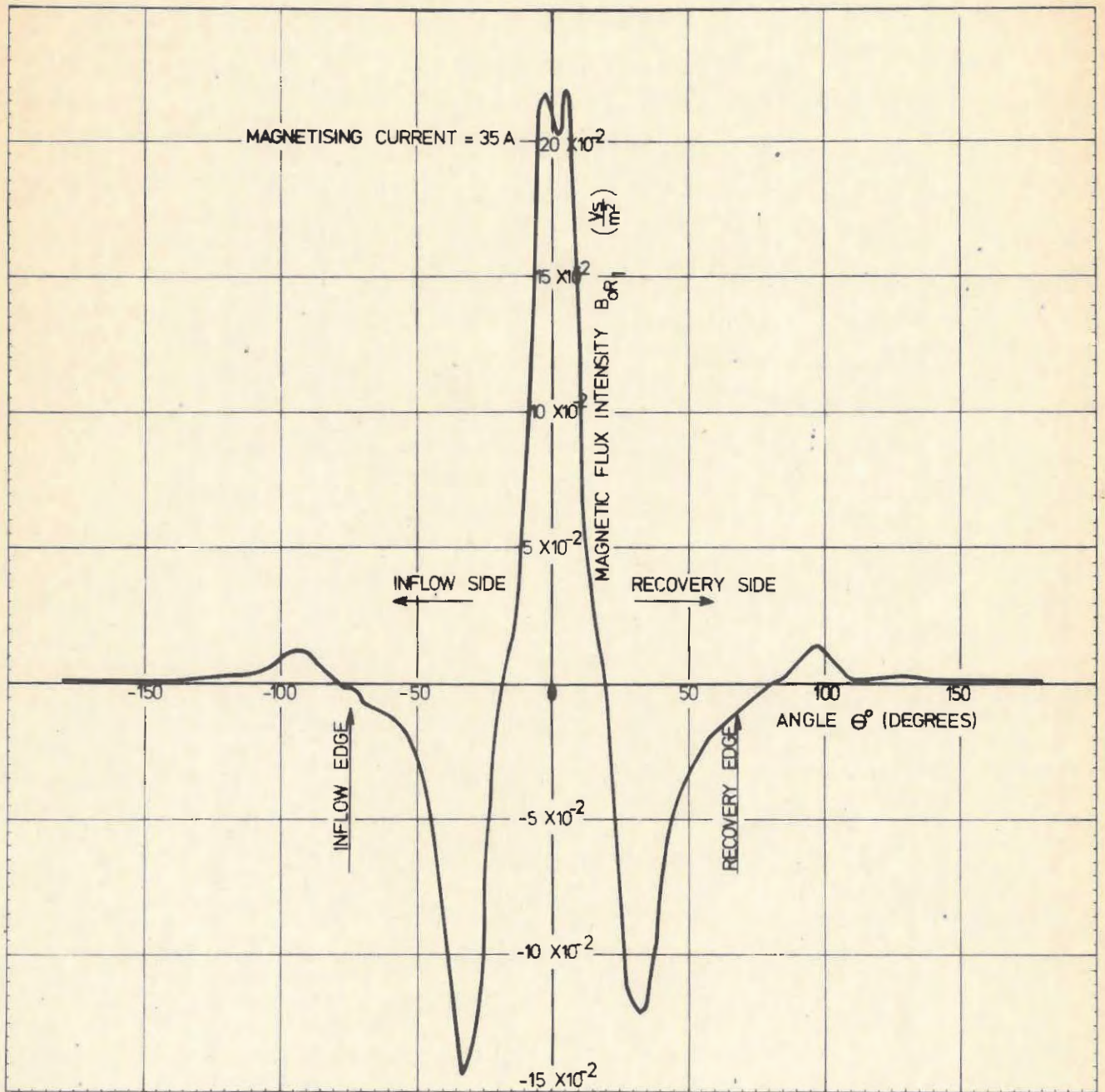
$\Delta R = R_3 - R_1 = 0,03 \text{ m}$

AXES OF THE MAGNETIC POLE PIECES.



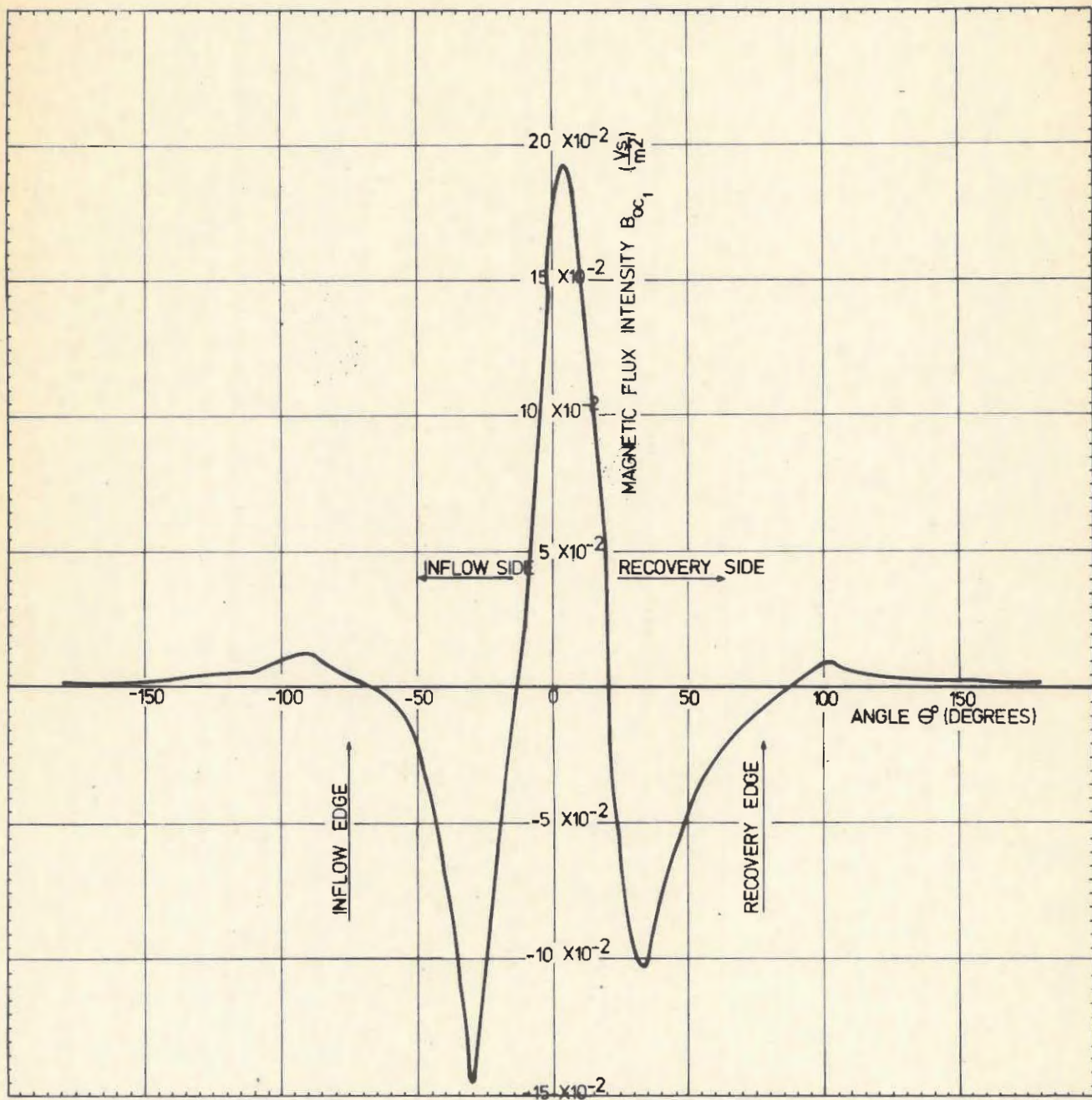
GEOMETRY AND CONVENTIONS OF THE MAGNETIC SEPARATOR

FIGURE 1



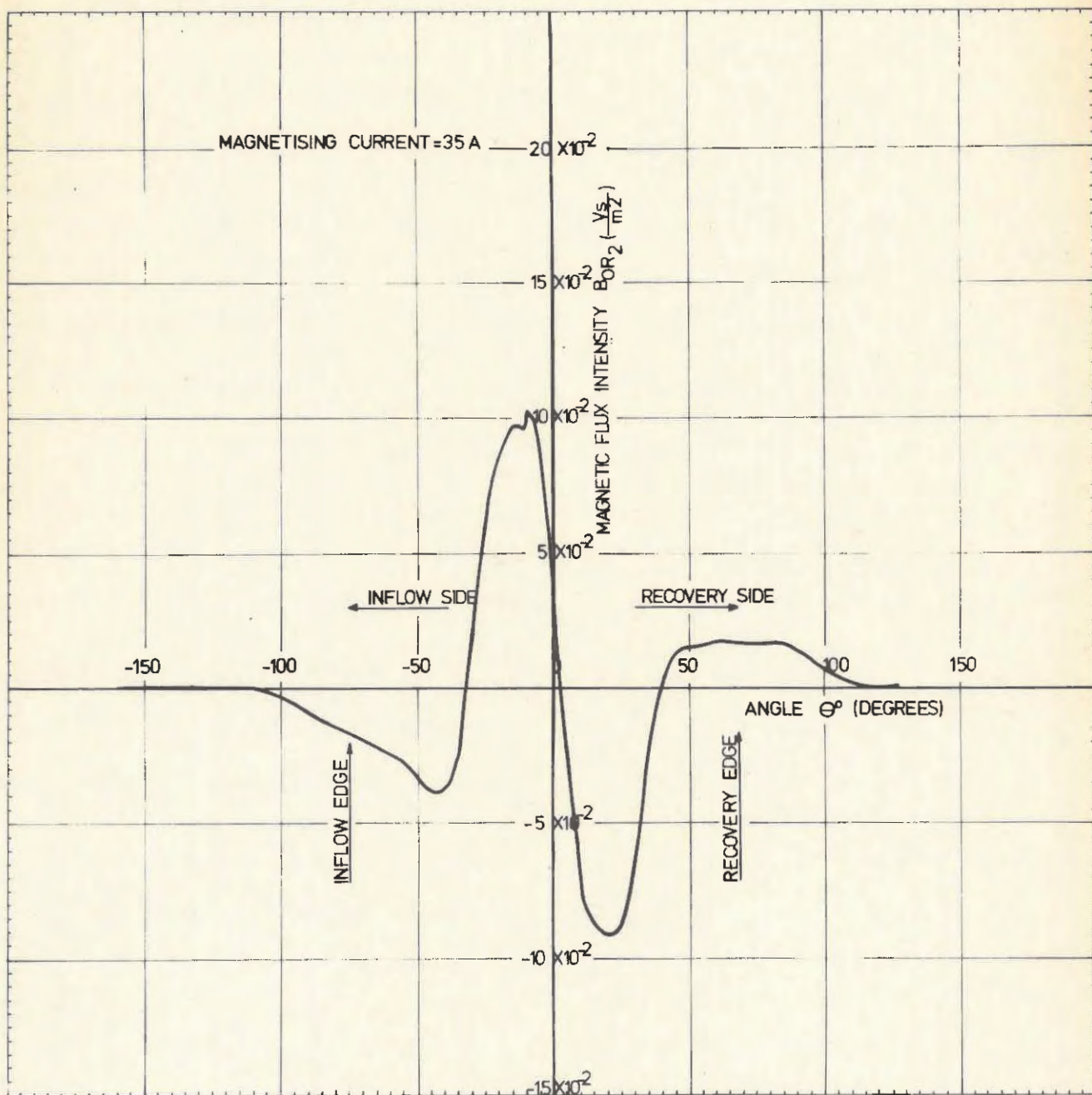
RADIAL COMPONENT OF MAGNETIC FLUX INTENSITY AT DRUM SURFACE ($R_1 = 0,3125$ m)

FIGURE 2.



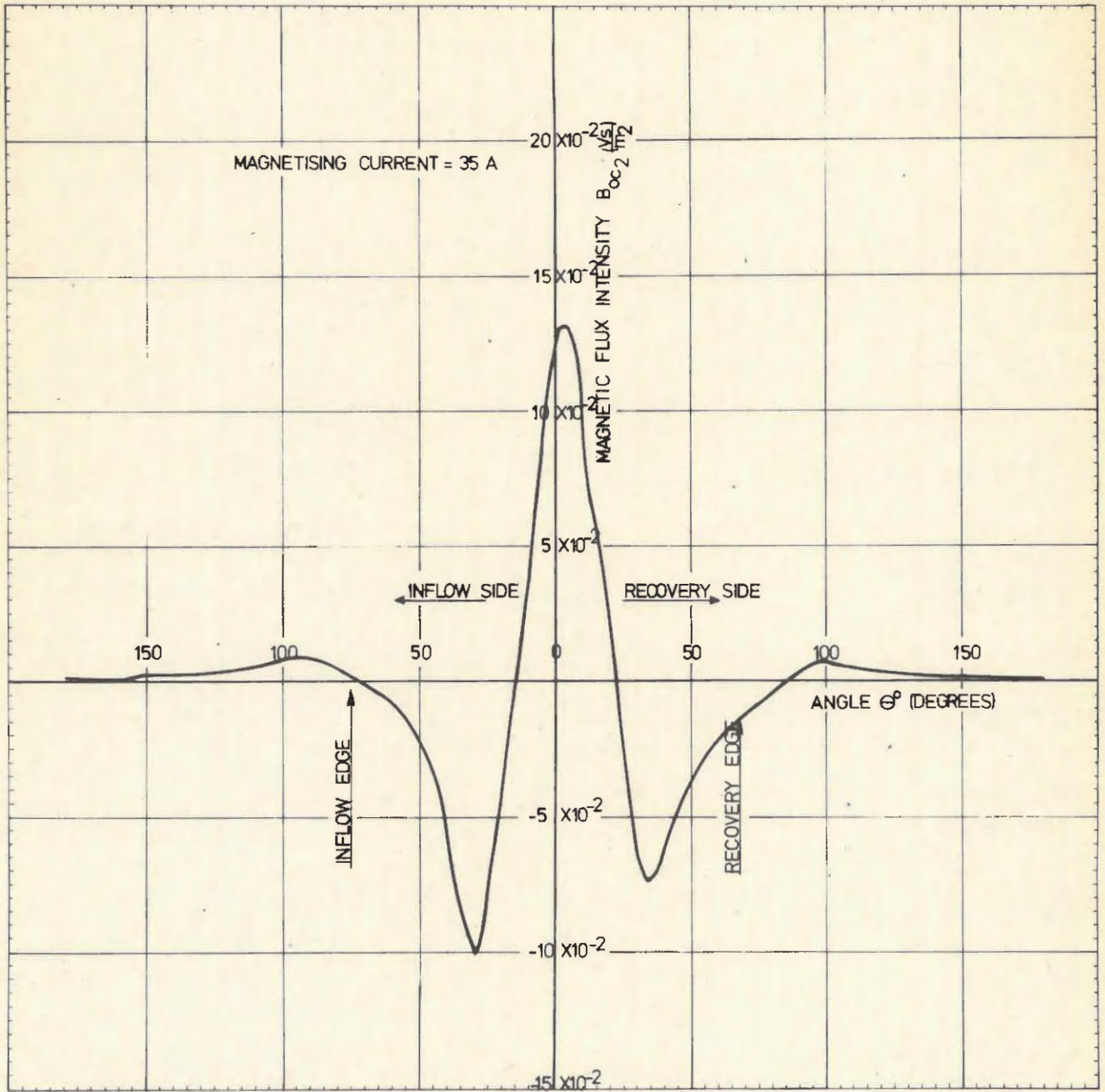
TANGENTIAL COMPONENT OF MAGNETIC FLUX INTENSITY AT DRUM SURFACE ($R_1 = 0,3125\text{m}$), EXTRAPOLATED.

FIGURE 3.



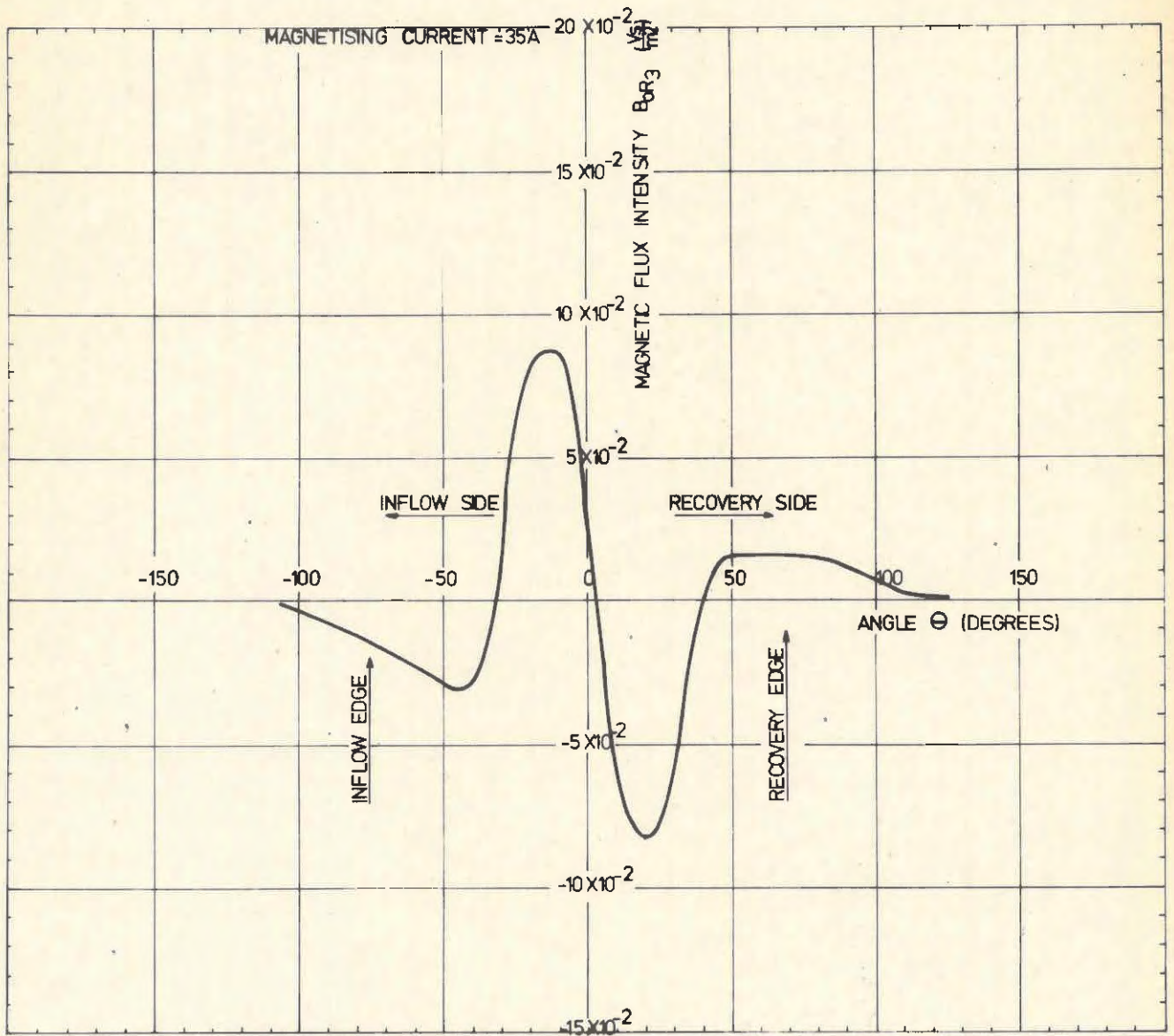
RADIAL COMPONENT OF MAGNETIC FLUX INTENSITY AT 20mm FROM DRUM SURFACE ($R_2 = 0,3325m$)

FIGURE 4



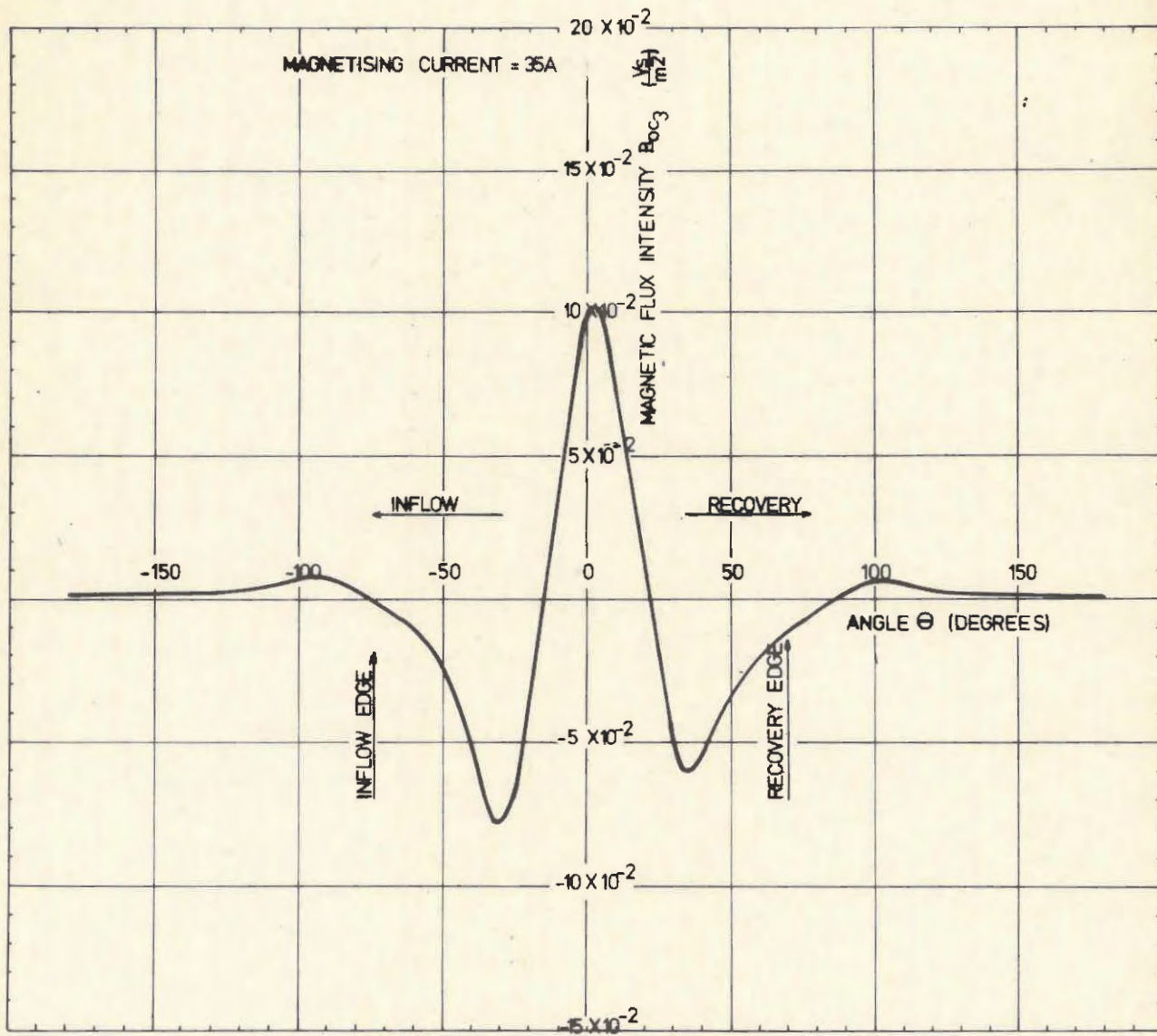
TANGENTIAL COMPONENT OF MAGNETIC FLUX INTENSITY AT 20mm FROM DRUM SURFACE ($R_2 = 0,3325\text{m}$)

FIGURE 5



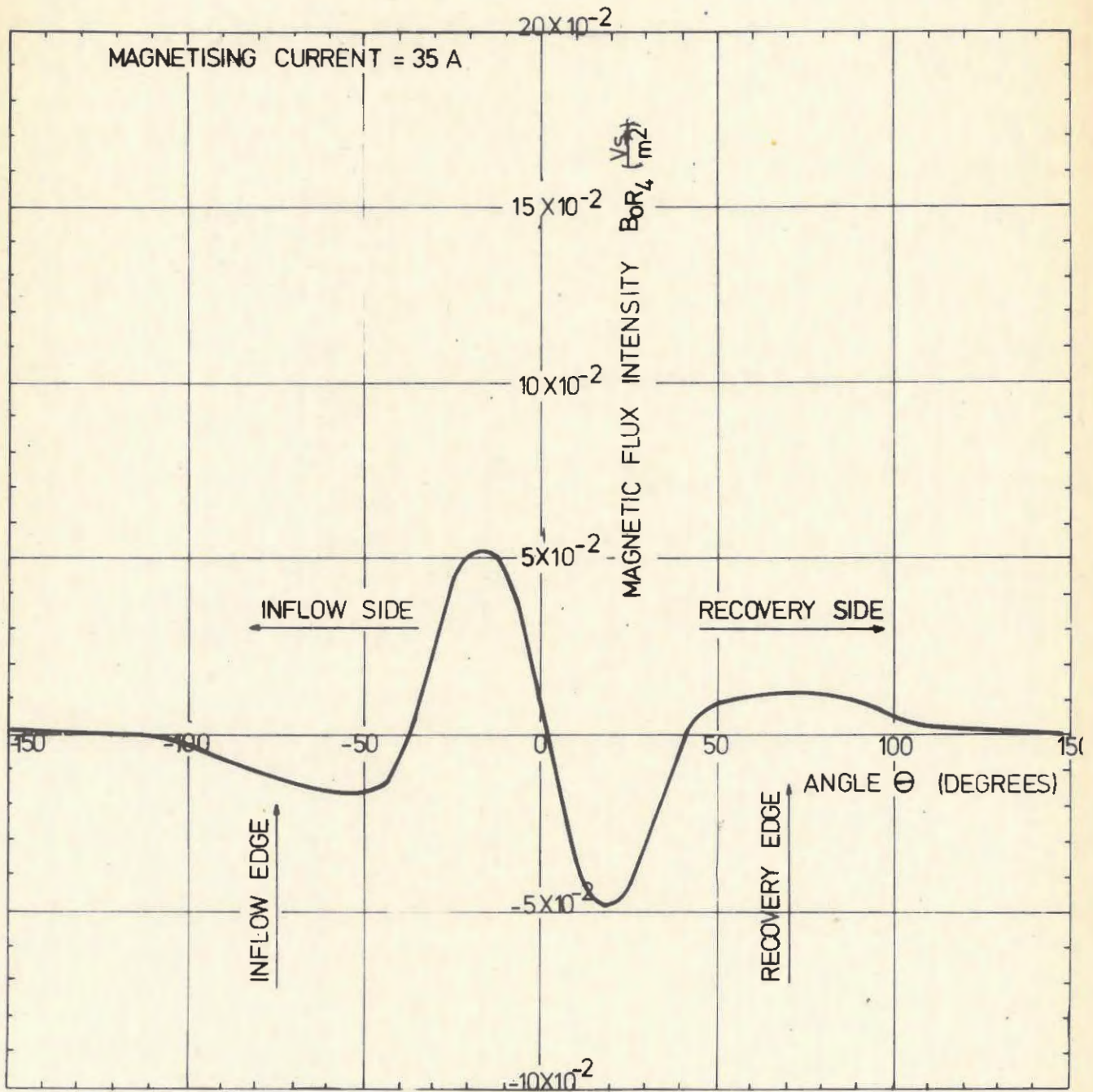
RADIAL COMPONENT OF THE MAGNETIC FLUX INTENSITY AT 30mm FROM DRUM SURFACE ($R_3 = 0,3425m$)

FIGURE 6



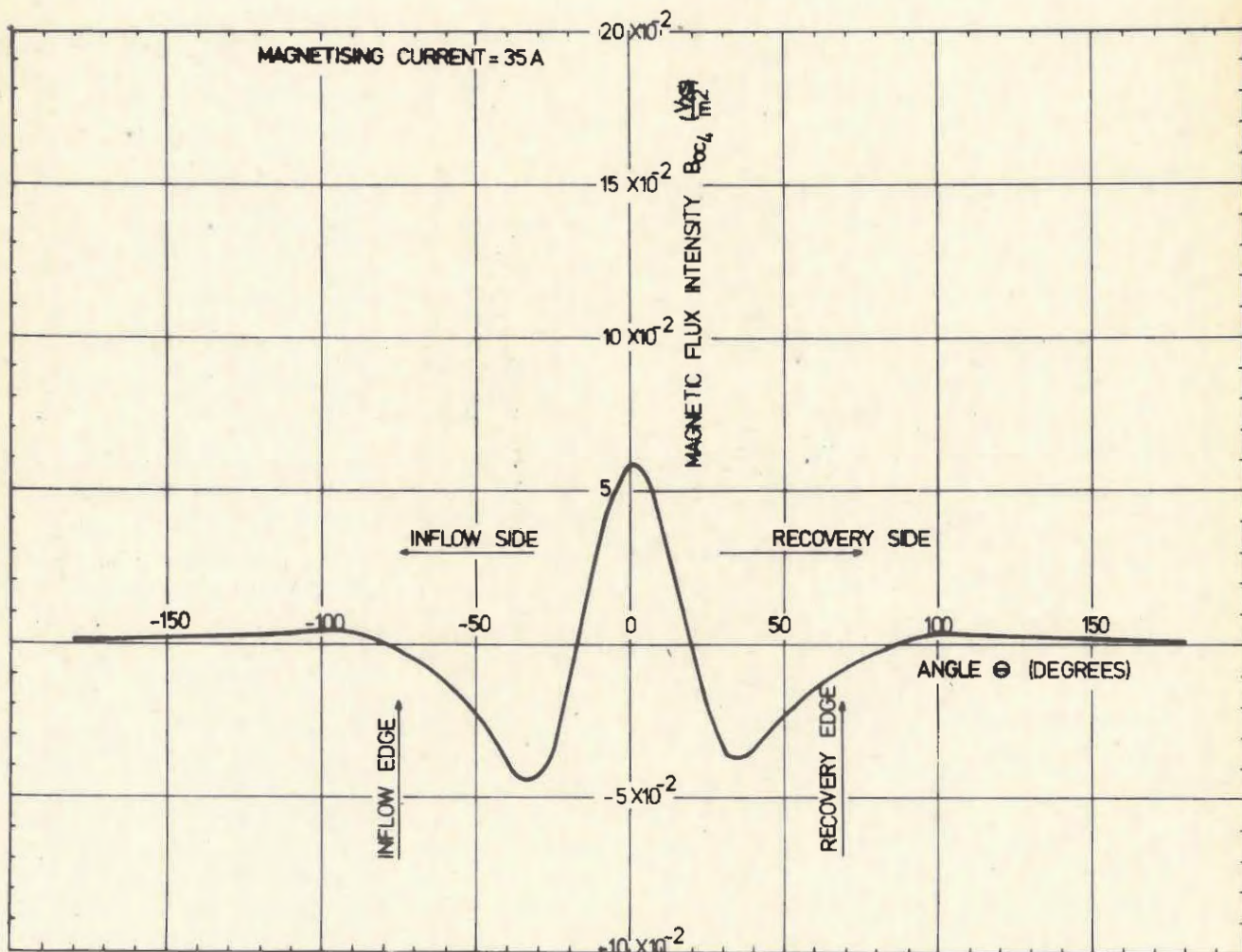
TANGENTIAL COMPONENT OF THE MAGNETIC FLUX INTENSITY AT 30mm FROM DRUM SURFACE ($R_3 = 0,3425$ m)

FIGURE 7



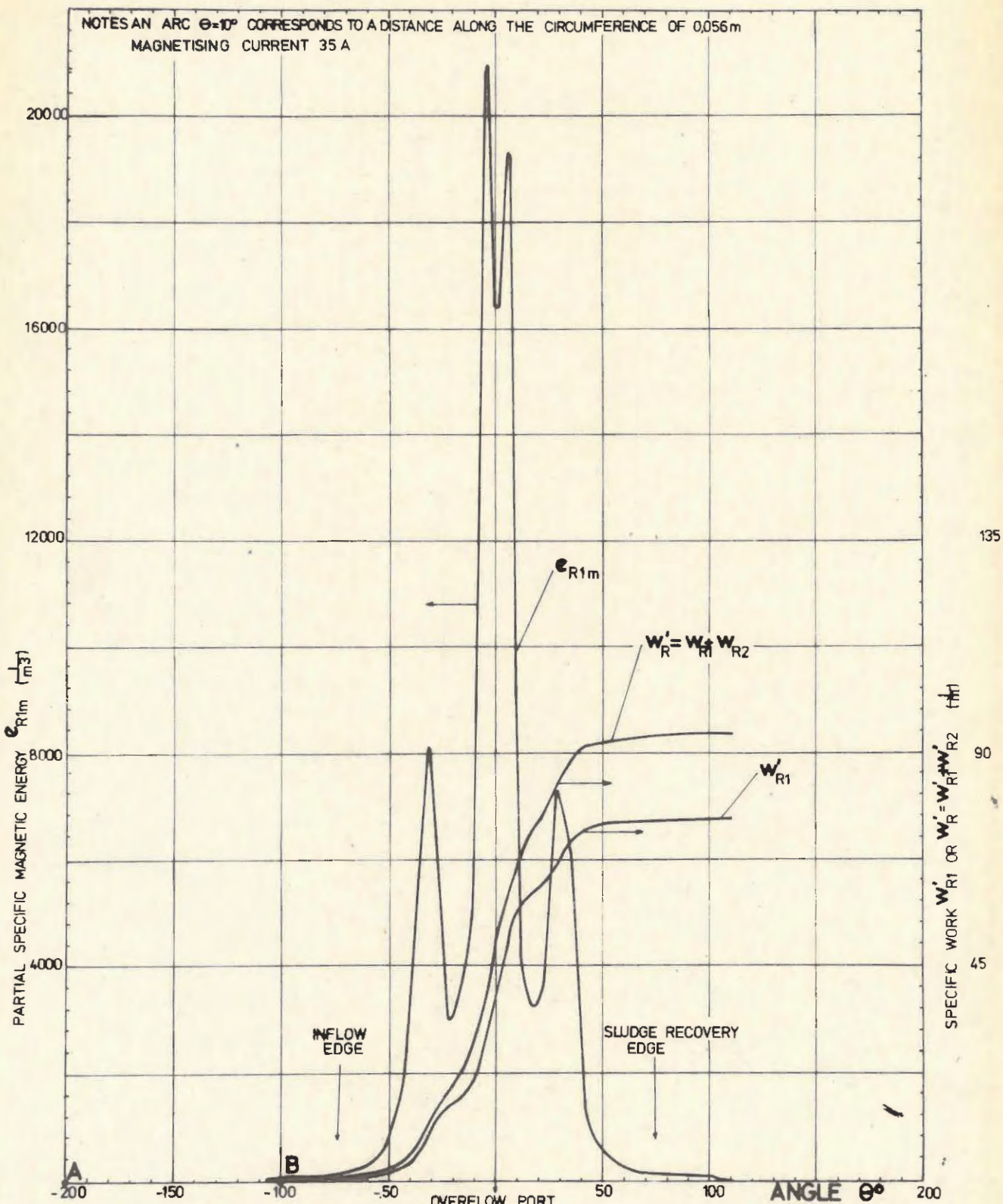
RADIAL COMPONENT OF THE MAGNETIC FLUX INTENSITY
AT 60mm FROM DRUM SURFACE ($R_4 = 0,3725$ m)

FIGURE 8

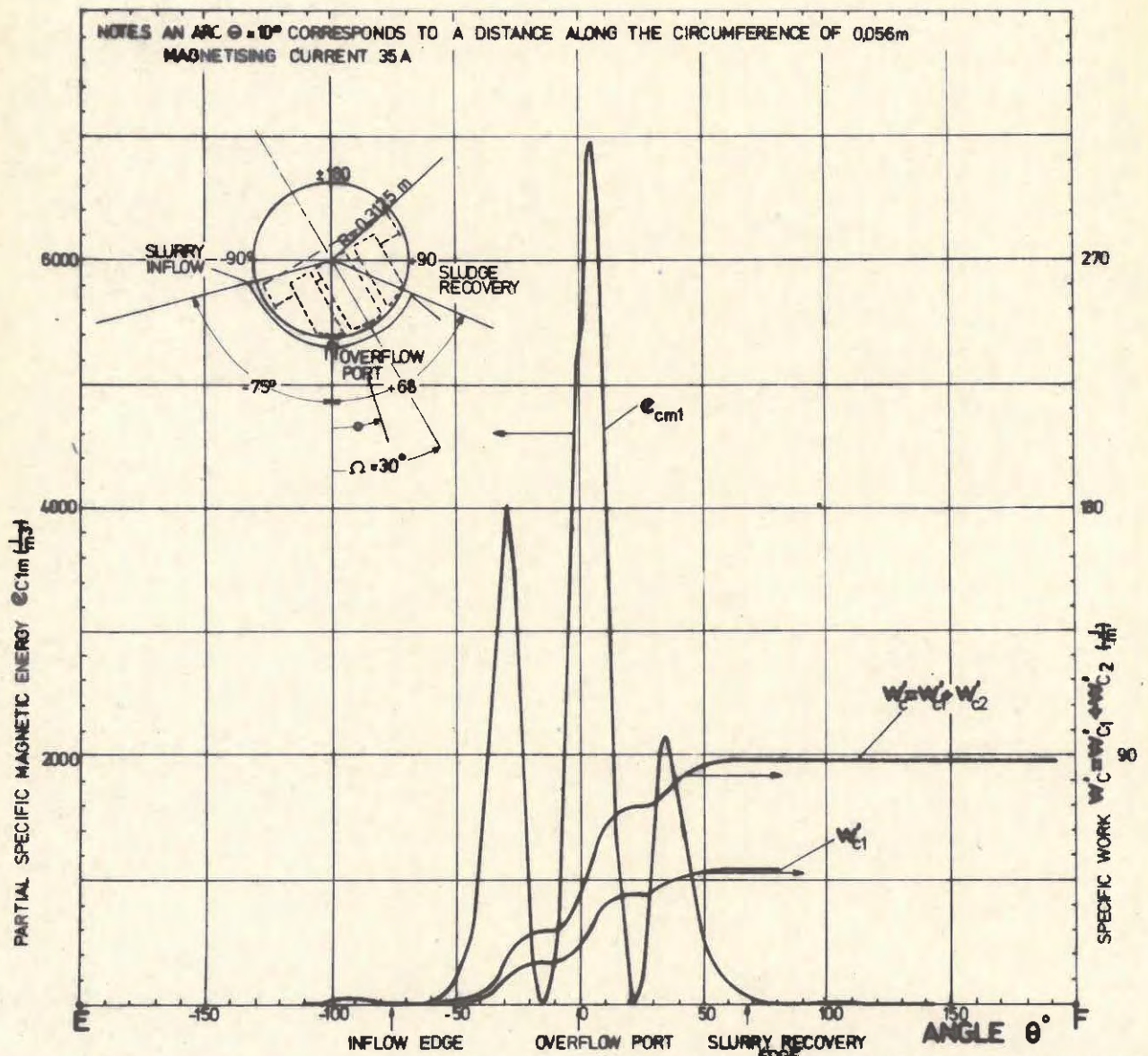


TANGENTIAL COMPONENT OF THE MAGNETIC FLUX INTENSITY AT 60 mm FROM DRUM SURFACE ($R_4 = 0,3725m$)

FIGURE 9

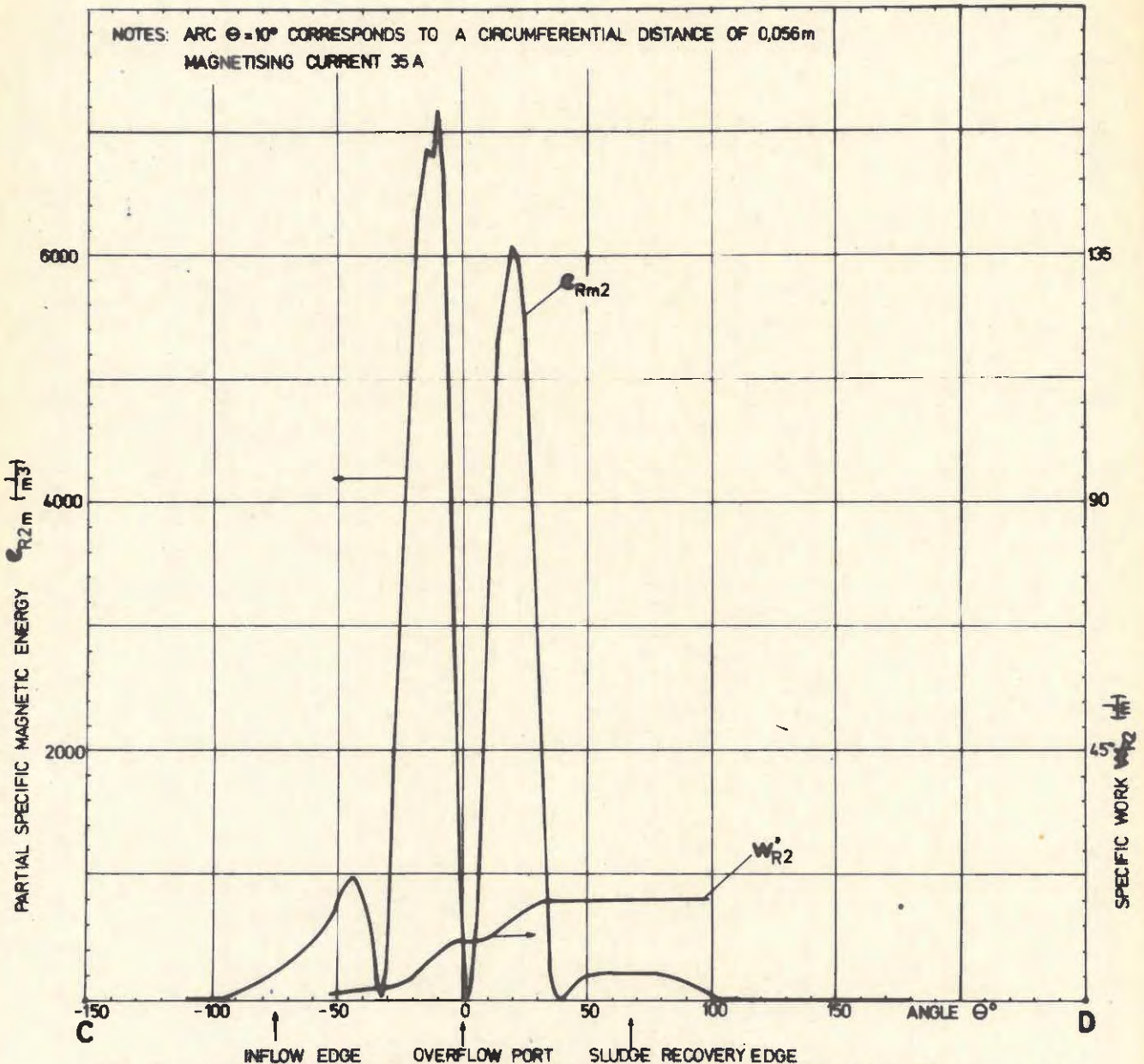


PARTIAL SPECIFIC MAGNETIC ENERGY e_{R1m} AND SPECIFIC WORK w_R IN RADIAL DIRECTION (e_{R1m} RELATIVE TO $R_{1m} = 0,3225m$) (w_R RELATIVE TO $\Delta R_1 = 0,02m$)
FIGURE 10



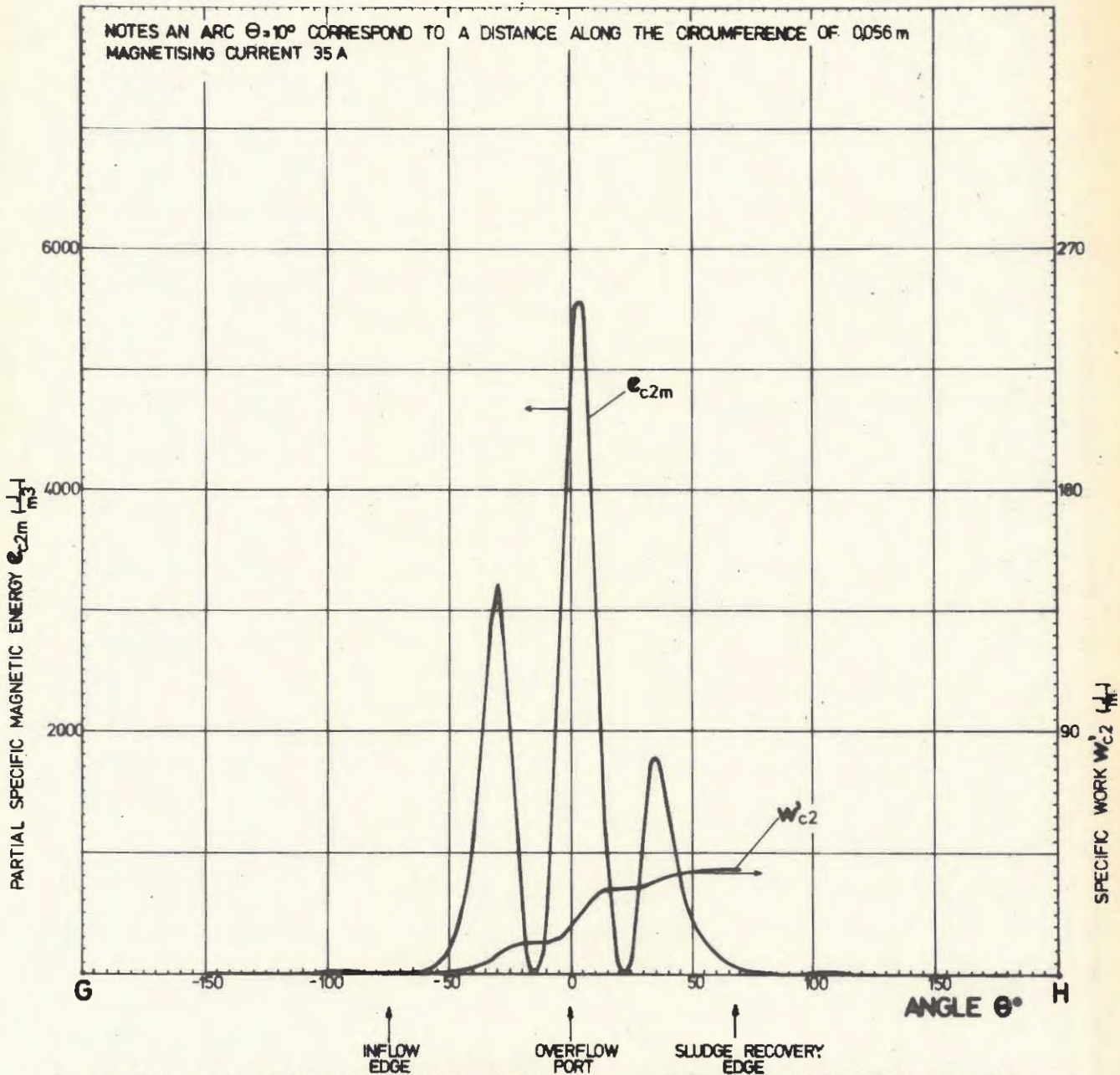
PARTIAL SPECIFIC MAGNETIC ENERGY e_{cm} AND SPECIFIC WORK w_c IN TANGENTIAL DIRECTION (e_{cm} RELATIVE TO $R_{tm} = 0,3225m$; w_c RELATIVE TO $\Delta R = 0,02m$)

FIGURE 11



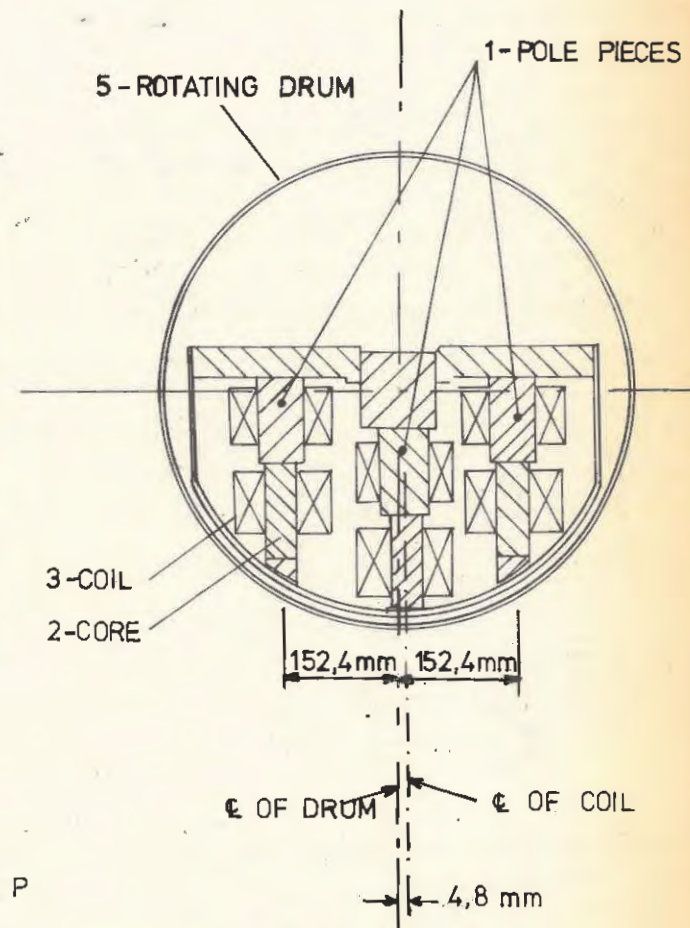
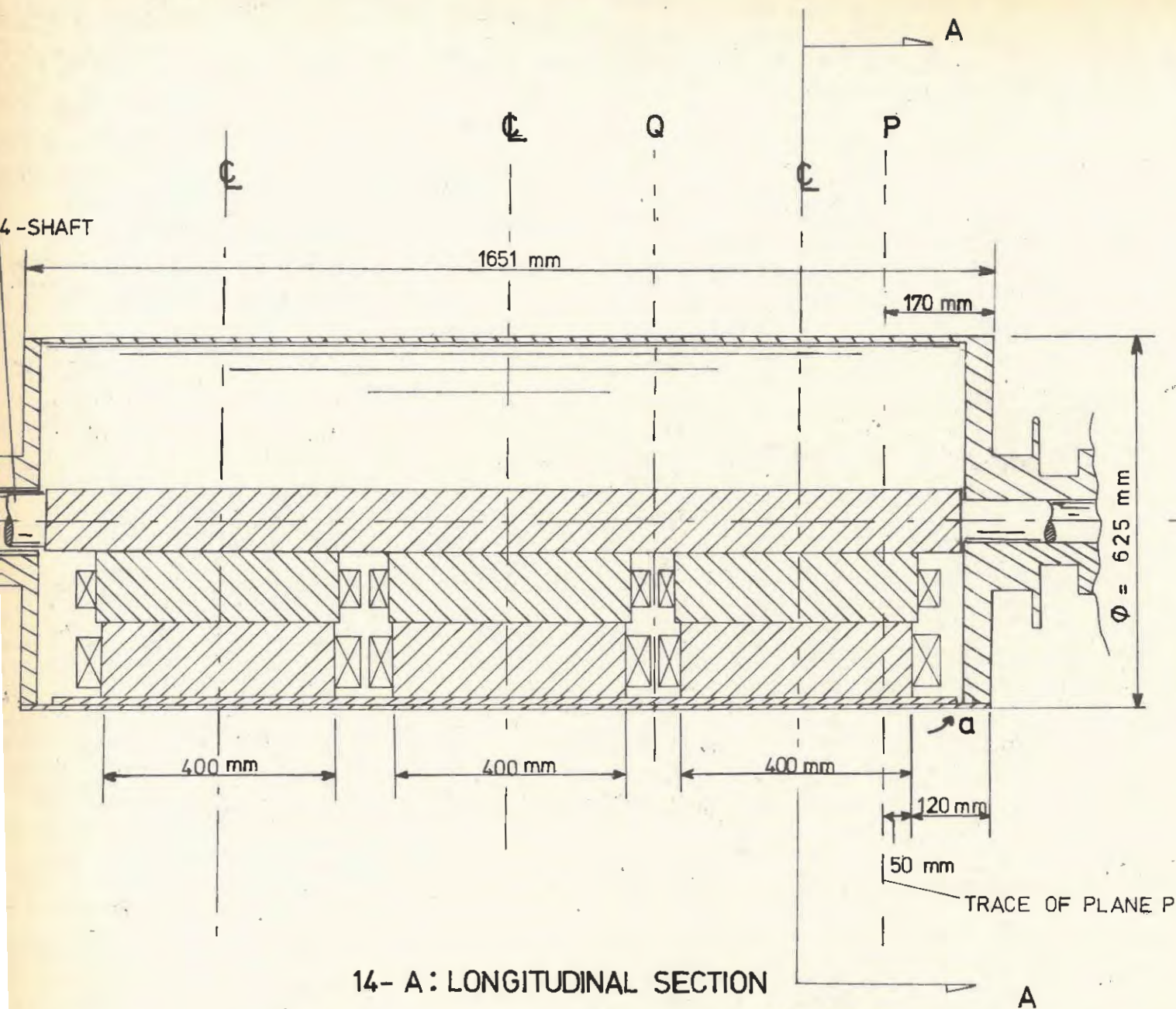
PARTIAL SPECIFIC MAGNETIC ENERGY e_{R2m} AND SPECIFIC WORK w'_{R2} IN RADIAL DIRECTION (e_{R2m} RELATIVE TO $R_{2m} = 0,3375m$; w'_{R2} RELATIVE TO $\Delta R_2 = 0,10m$)

FIGURE 12



PARTIAL SPECIFIC MAGNETIC ENERGY e_{c2m} AND SPECIFIC WORK w_{c2} IN TANGENTIAL DIRECTION (e_{c2m} RELATIVE TO $R_{2m} = 0,3375m$; w_{c2} RELATIVE TO $\Delta R = 0,10m$)

FIGURE 13



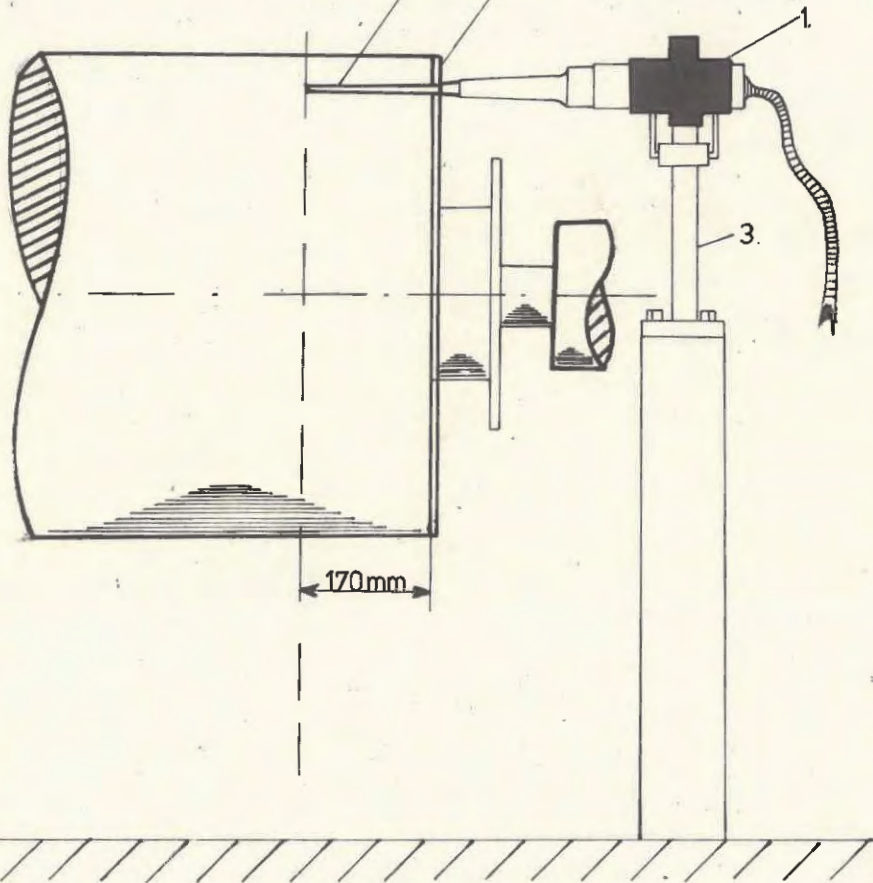
LAY-OUT OF MAGNET

FIGURE 14

Plane P.

Instrument Probe

4-Graduated Quadrant.



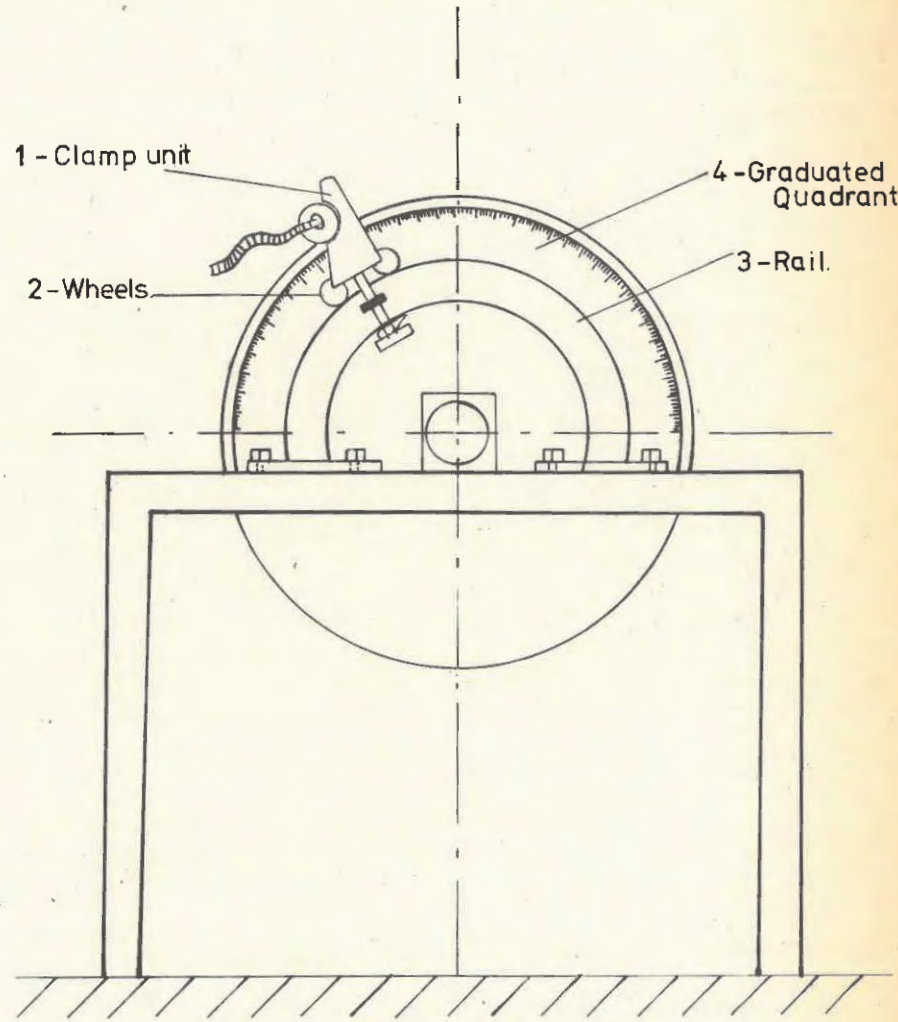
15-A LONGITUDINAL VIEW

1 - Clamp unit

2 - Wheels

4 - Graduated Quadrant

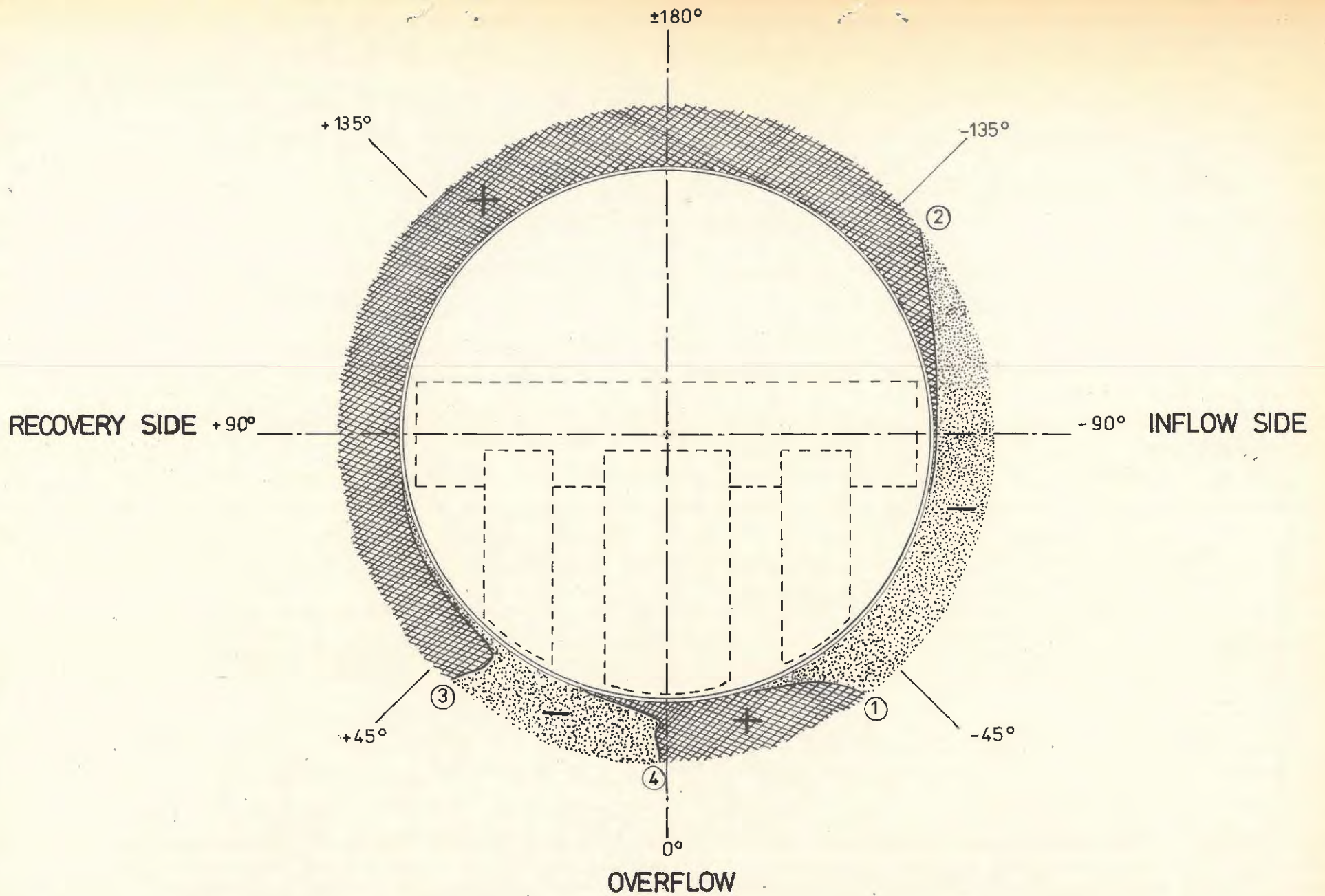
3 - Rail.



15-B SIDE VIEW

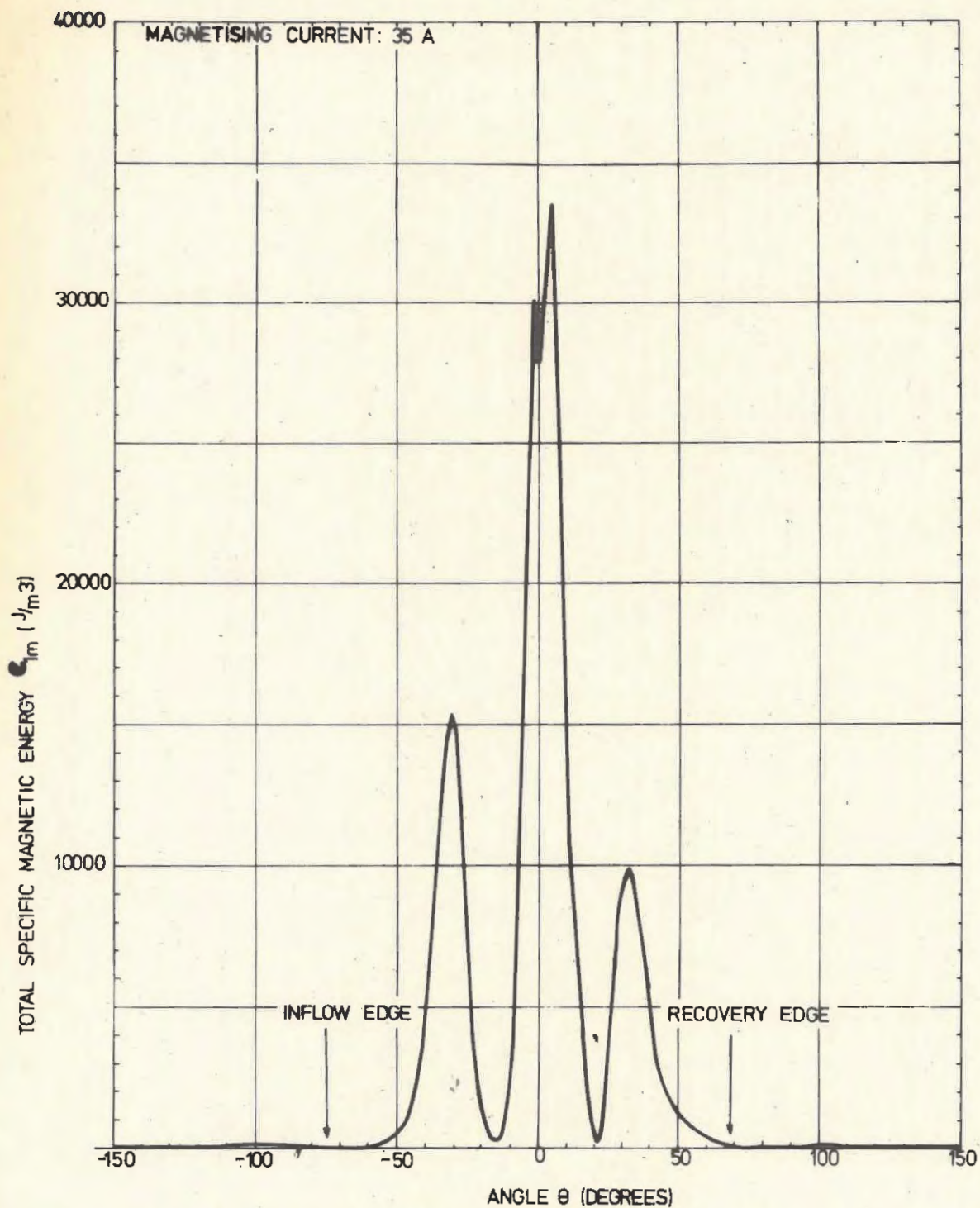
MEASURING RIG

FIGURE 15



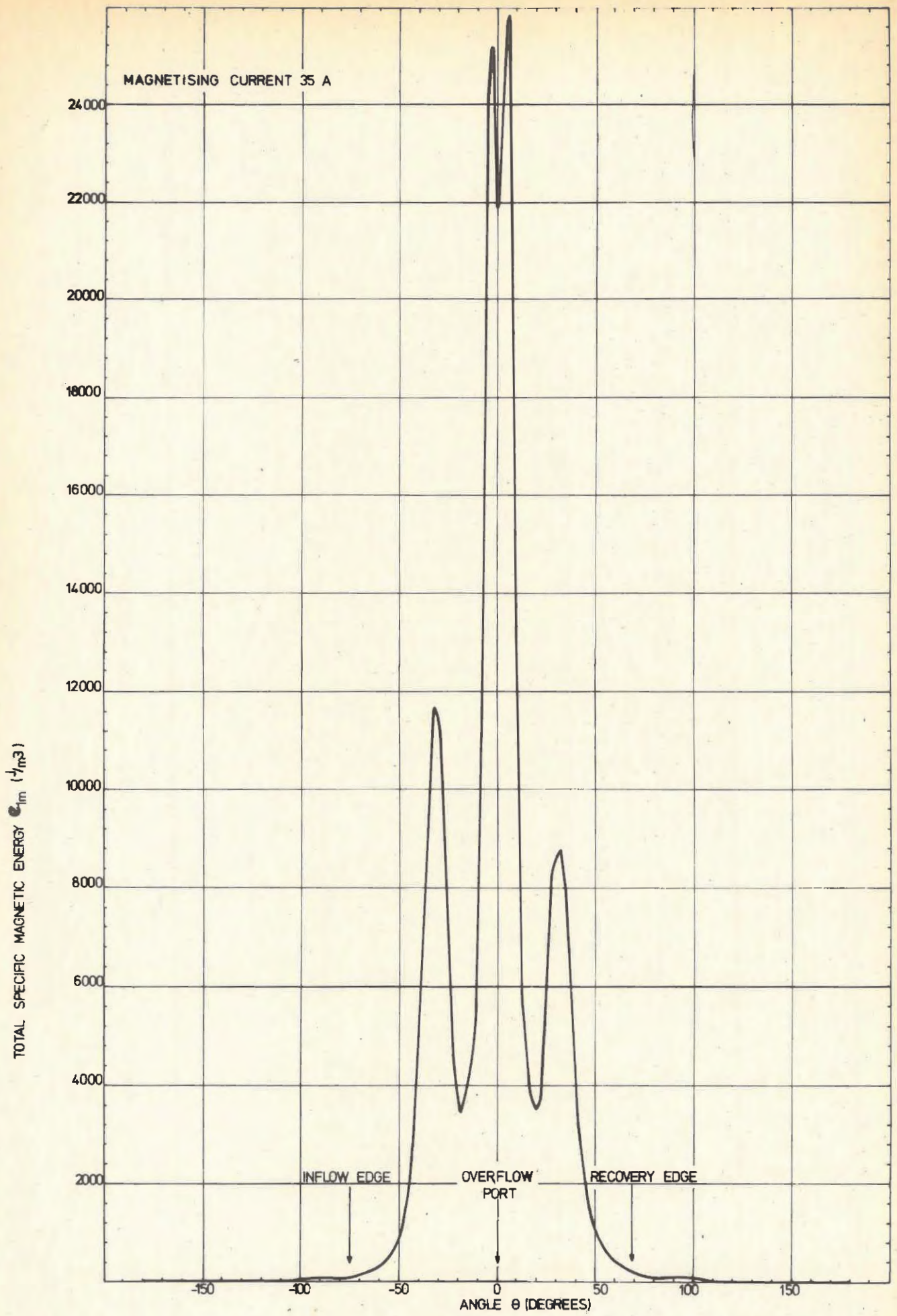
DISTRIBUTION OF EFFECTIVE MAGNETIC FIELD IN RADIAL DIRECTION

FIGURE 16



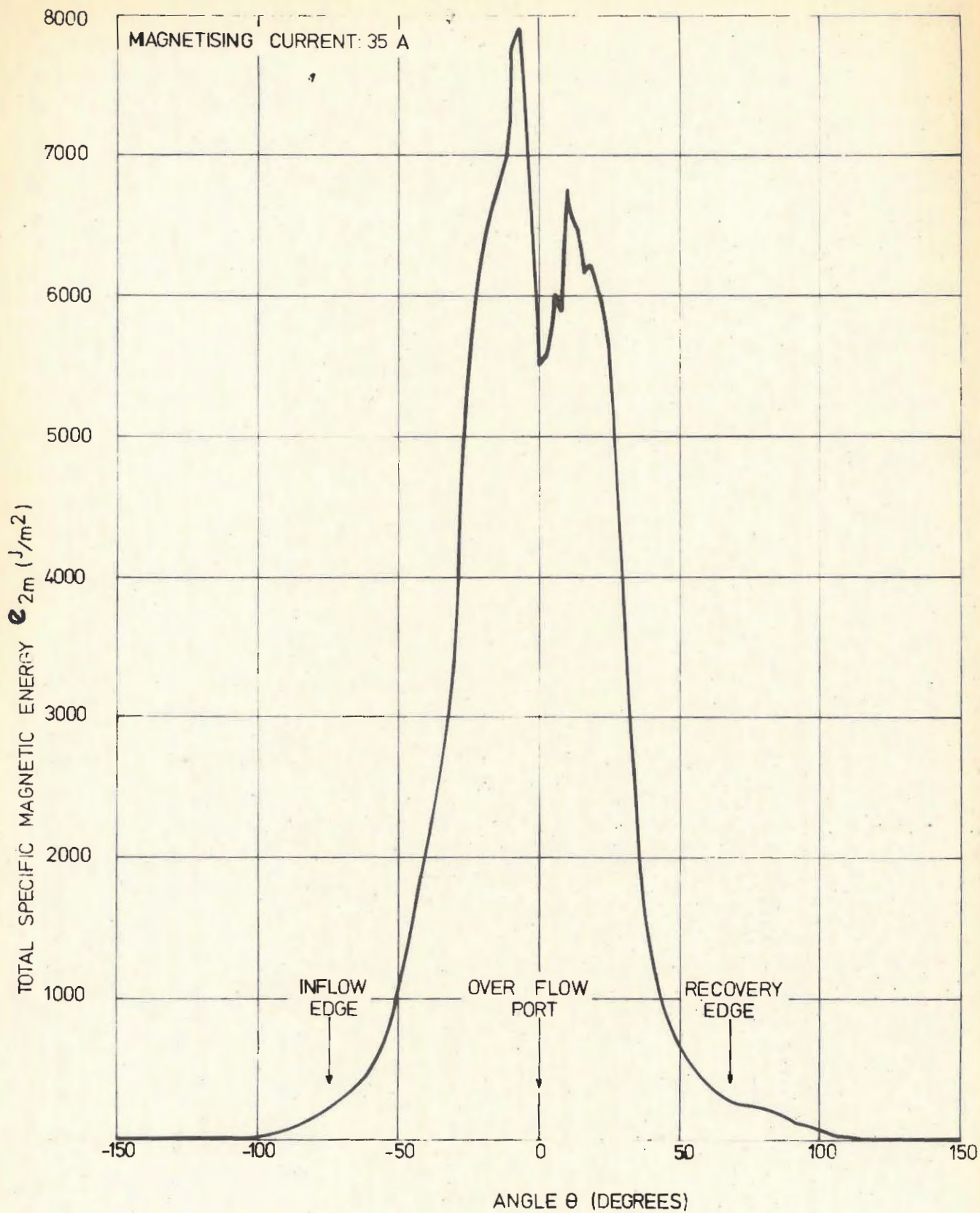
TOTAL SPECIFIC MAGNETIC ENERGY e_m , AT THE DRUM SURFACE
 $R_1 = 0,3125$ m.

FIGURE 17



TOTAL SPECIFIC MAGNETIC ENERGY ϵ_{lm} RELATIVE TO $R_{lm} = 0,3225m$

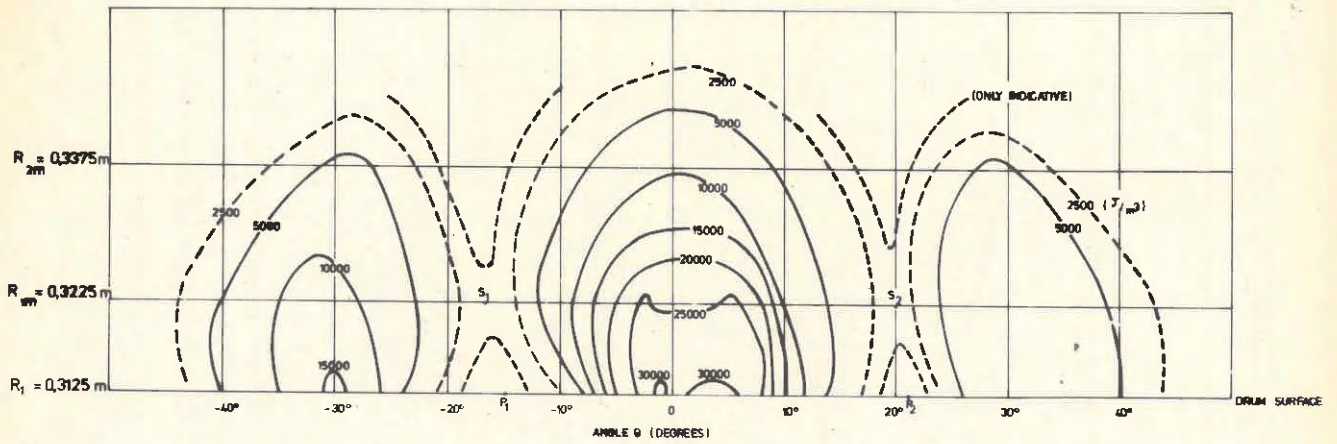
FIGURE 18



TOTAL SPECIFIC MAGNETIC ENERGY e_{2m} , RELATIVE TO
 $R_{2m} = 0,3375m$

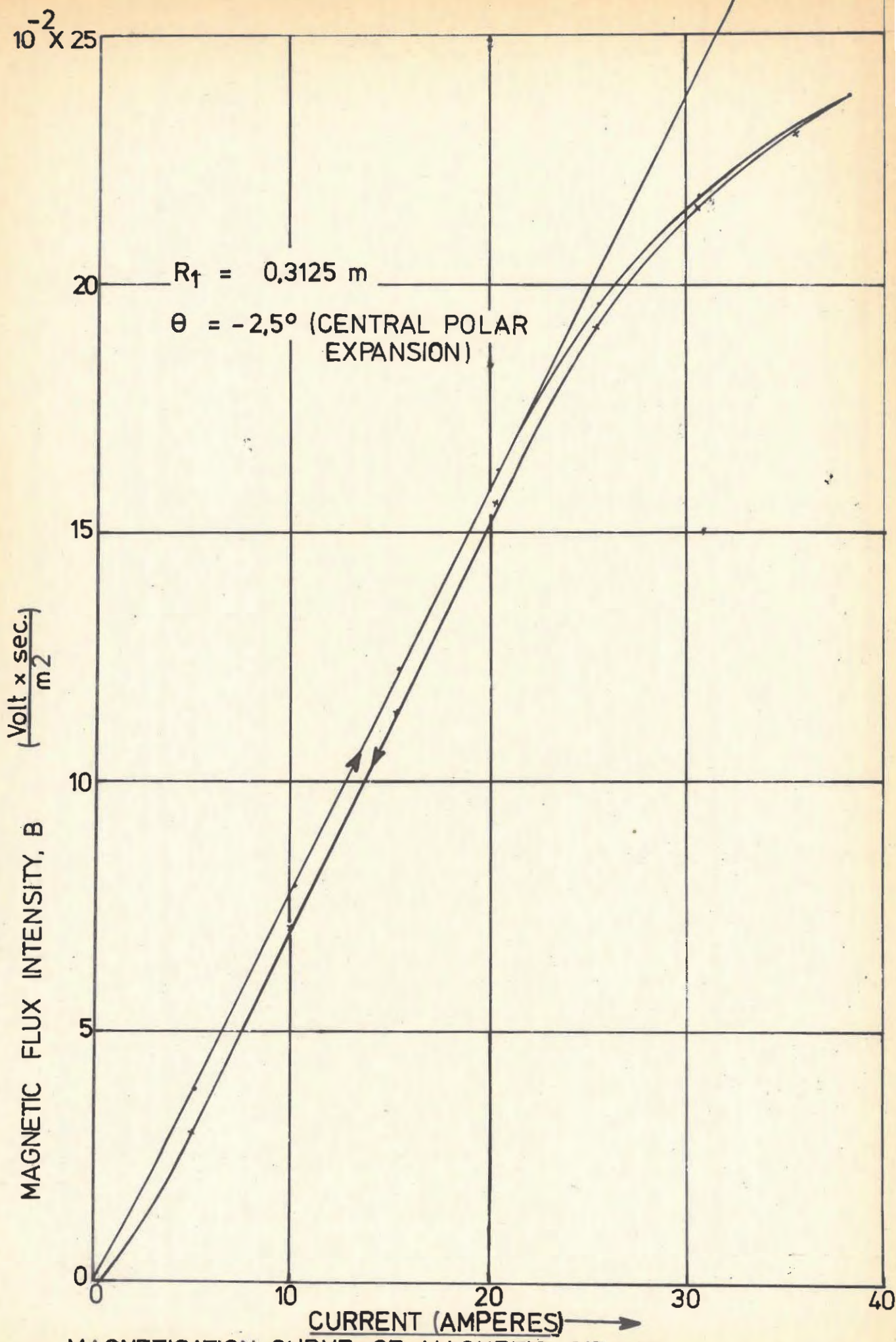
FIGURE 19

NOTES: S_1 AND S_2 ARE SADDLE POINTS OF THE MAGNETIC ENERGY RELIEF BODY.
 NUMERICAL VALUES NEXT TO EQUIPOTENTIAL LINES ARE EXPRESSED IN $\frac{J}{m^3}$
 MAGNETISING CURRENT: 35 A



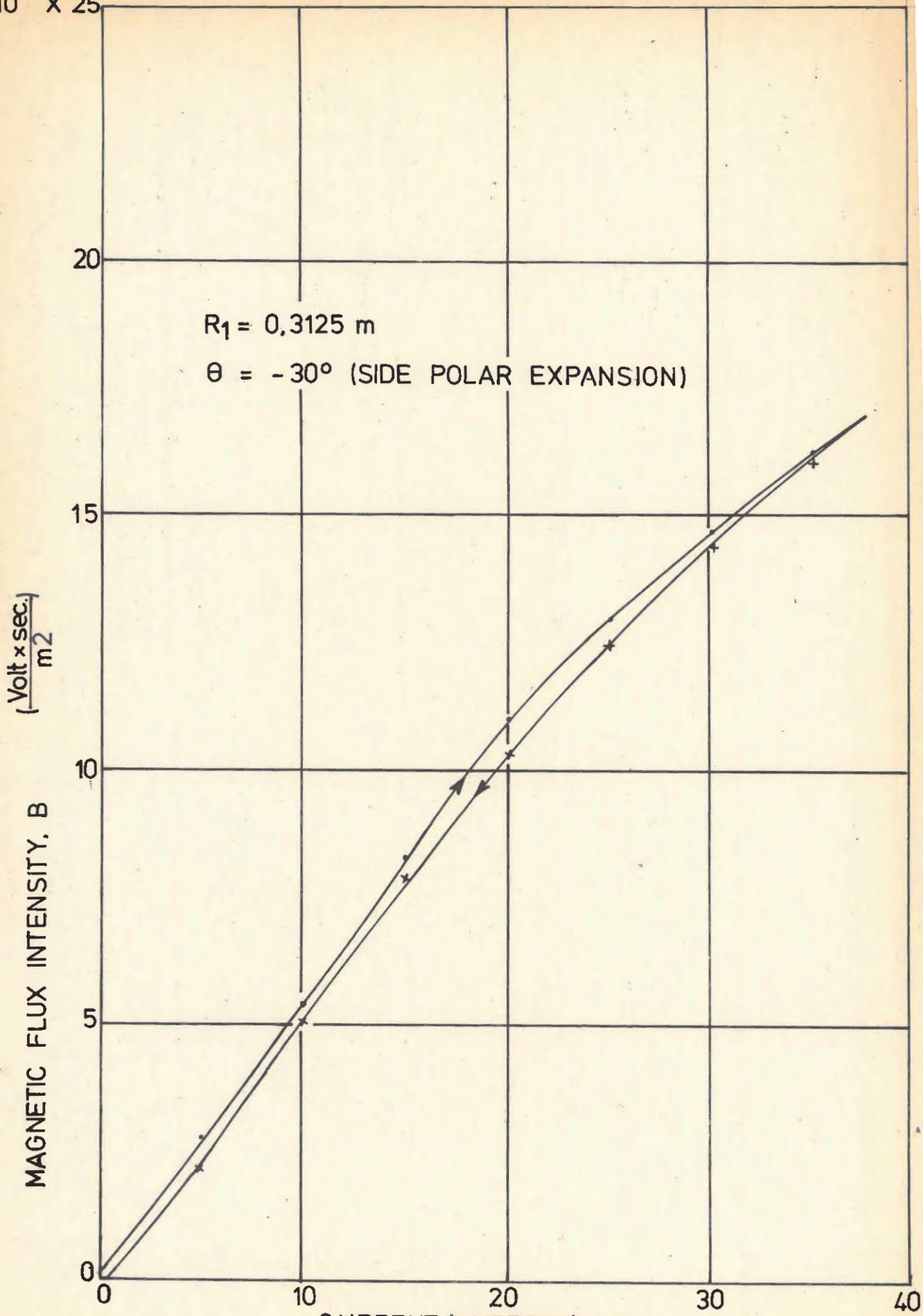
REPRESENTATION OF THE MAGNETIC ENERGY FIELD INSIDE THE ANGULAR SPACE BY MEANS OF EQUIPOTENTIAL LINES

FIGURE 20



MAGNETISATION CURVE OF MAGNETIC CIRCUIT
 FIGURE 21

$10^{-2} \times 25$



MAGNETISATION CURVE OF MAGNETIC CIRCUIT
FIGURE 22

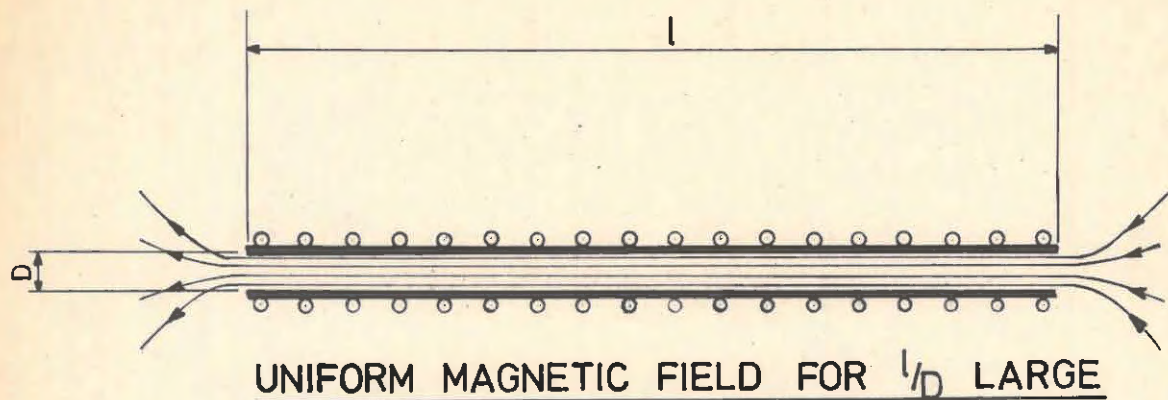
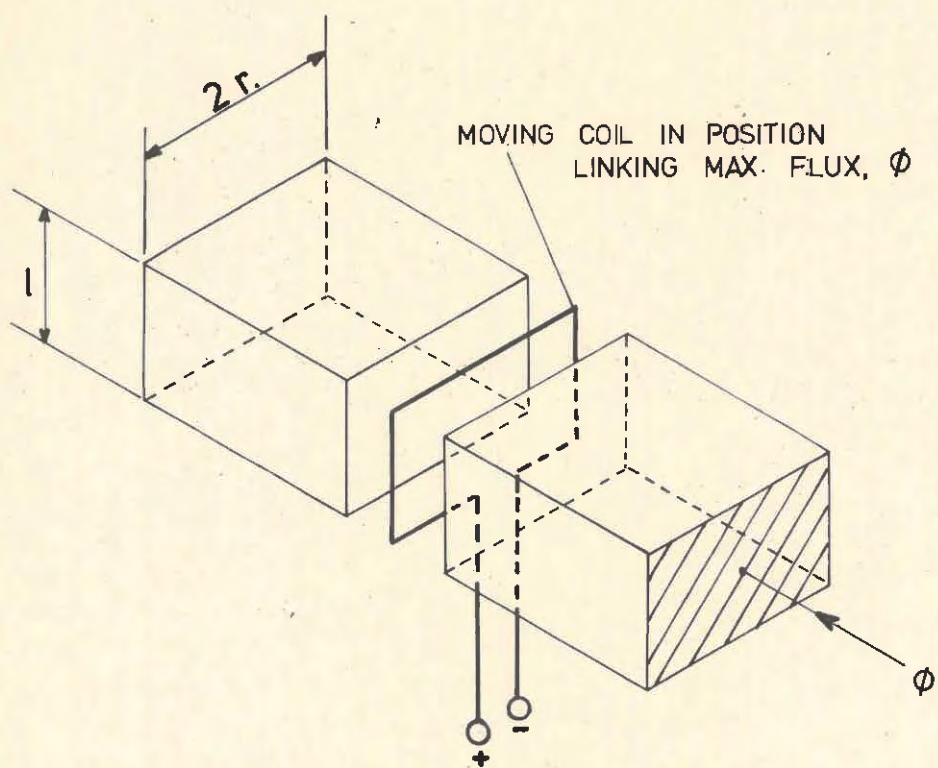


FIGURE 23



MOVING COIL IN A UNIFORM MAGNETIC FIELD

FIGURE 24